Particle Cosmology

FRW Cosmology
Inflation
Baryogenesis
Big Bang Nucleosynthesis

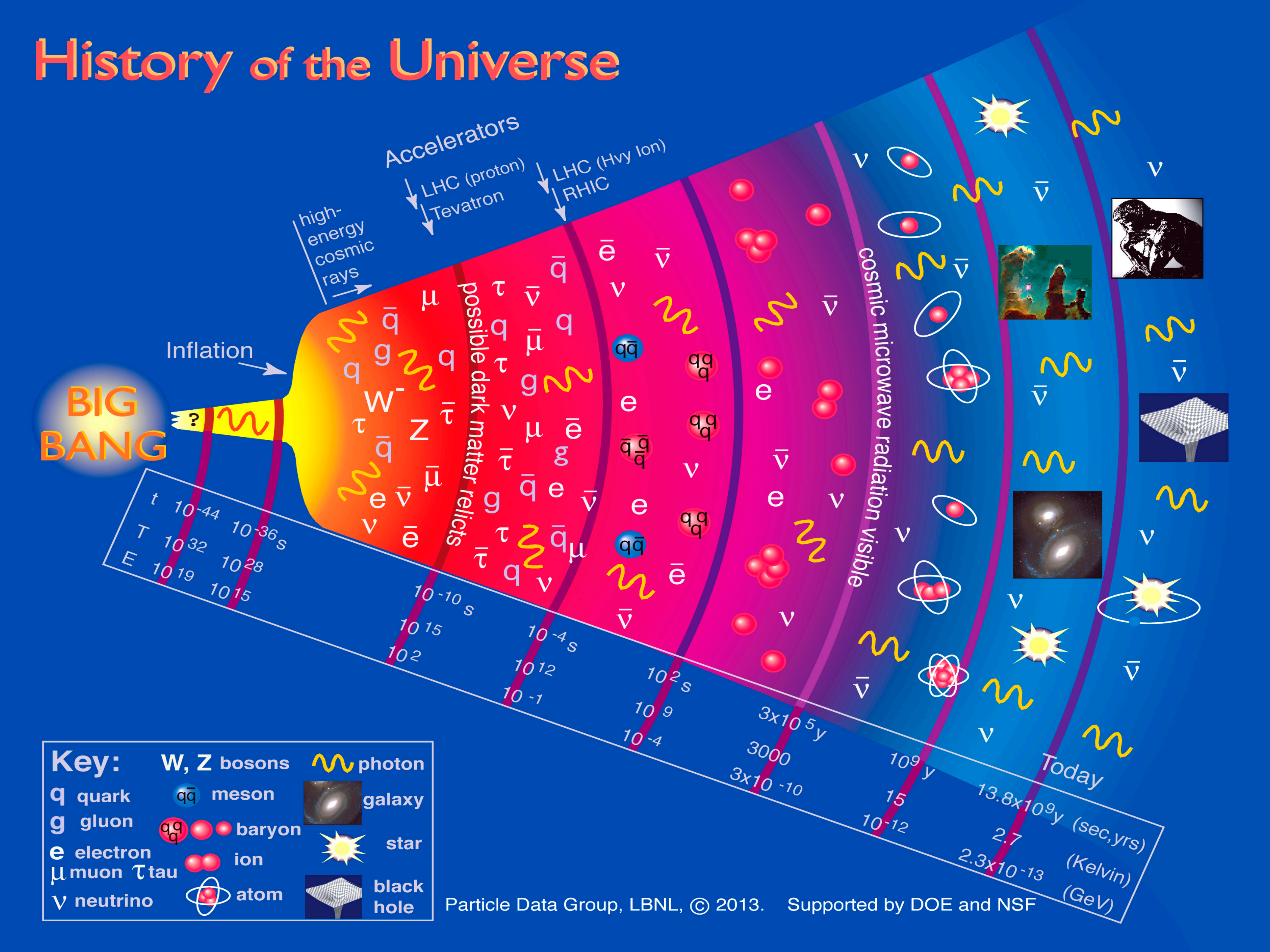
History of the Universe
Accelerators
LHC (proton)
Tevatron
LHC (Hvy Ion)
RHIC
high-energy cosmic rays
Inflation
BIG BANG
possible dark matter relicts
cosmic microwave radiation visible
Today
t 10^{-44} 10^{-36} s
T 10^{32} 10^{28}
E 10^{19} 10^{15}
10^{-10} s
10^{15}
10^{2}
10^{-4} s
10^{12}
10^{-1}
10^{2} s
10^{9}
10^{-4}
$3x10^{5}$ y
3000
$3x10^{-10}$
10^{9} y
15
10^{-12}
$13.8x10^{9}$ y (sec,yrs)
2.7 (Kelvin)
$2.3x10^{-13}$ (GeV)
Key:
W, Z bosons
photon
q quark
meson
galaxy
g gluon
baryon
star
e electron
ion
μ muon τ tau
ν neutrino
atom
black hole
Particle Data Group, LBNL, © 2013. Supported by DOE and NSF

Big Bang Nucleosynthesis

- BBN and the WMAP/Planck determination of η, $\Omega_B h^2$
- Input cross sections

- Observations and Comparison with Theory

  - D/H - ^{4}He - ^{7}Li

- Neutrinos
- Constraints on BSM physics
- The Future (CMB)

Foundations of Big Bang Cosmology: Nucleosynthesis and the CMB

Big Bang cosmology grew from the work of Gamow, Alpher, and Hermann in their attempts to explain the observed element abundances.

They predicted the existence of the 3K background which was discovered 16 years later.

It all started with:

George Gamow

Ralph Alpher

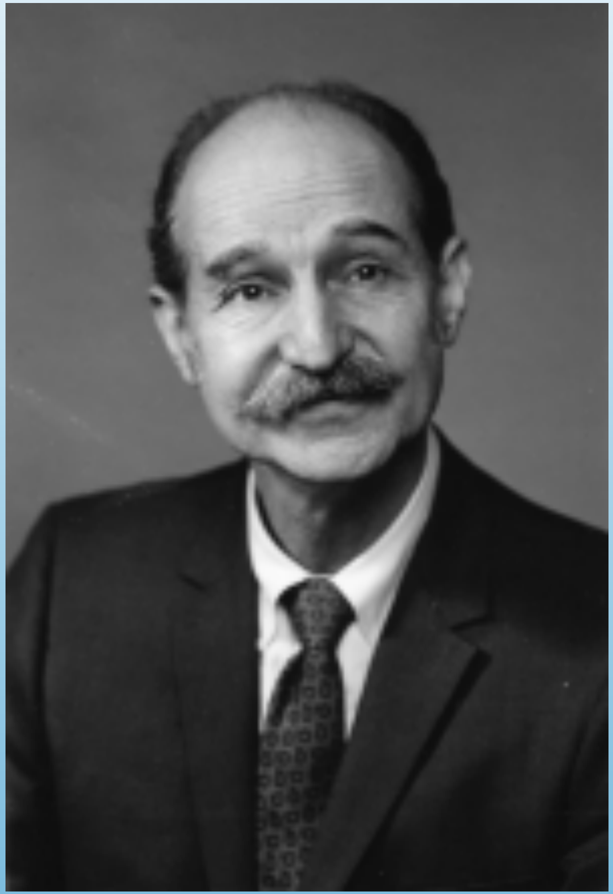

Robert Herman

It all started with:

Ralph Alpher

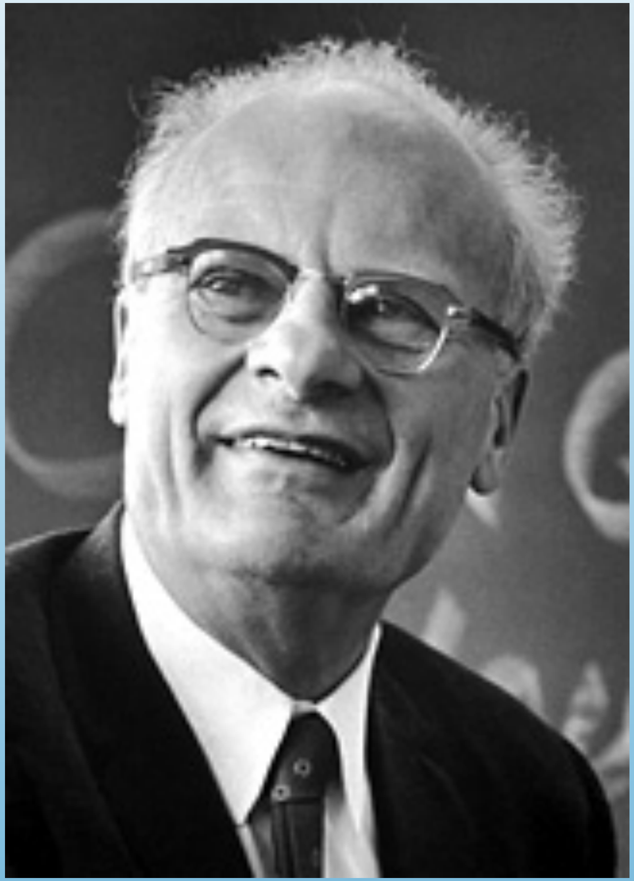

Hans Bethe

George Gamow

Letters to the Editor

PUBLICATION of brief reports of important discoveries in physics may be secured by addressing them to this department. The closing date for this department is five weeks prior to the date of issue. No proof will be sent to the authors. The Board of Editors does not hold itself responsible for the opinions expressed by the correspondents. Communications should not exceed 600 words in length.

The Origin of Chemical Elements

R. A. ALPHER*
Applied Physics Laboratory, The Johns Hopkins University, Silver Spring, Maryland

AND

H. BETHE
Cornell University, Ithaca, New York

AND

G. GAMOW
The George Washington University, Washington, D. C.
February 18, 1948

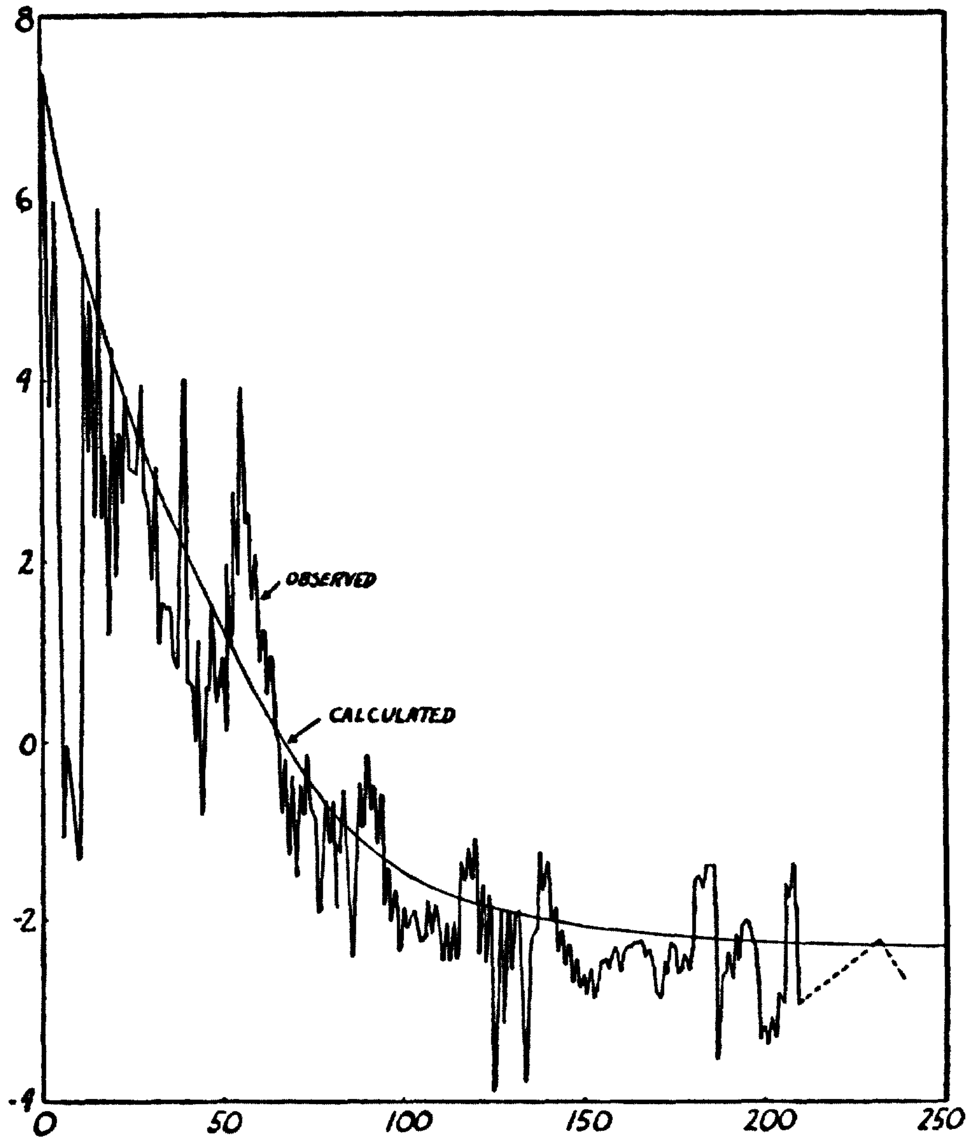

FIG. 1.

Log of relative abundance

Atomic weight

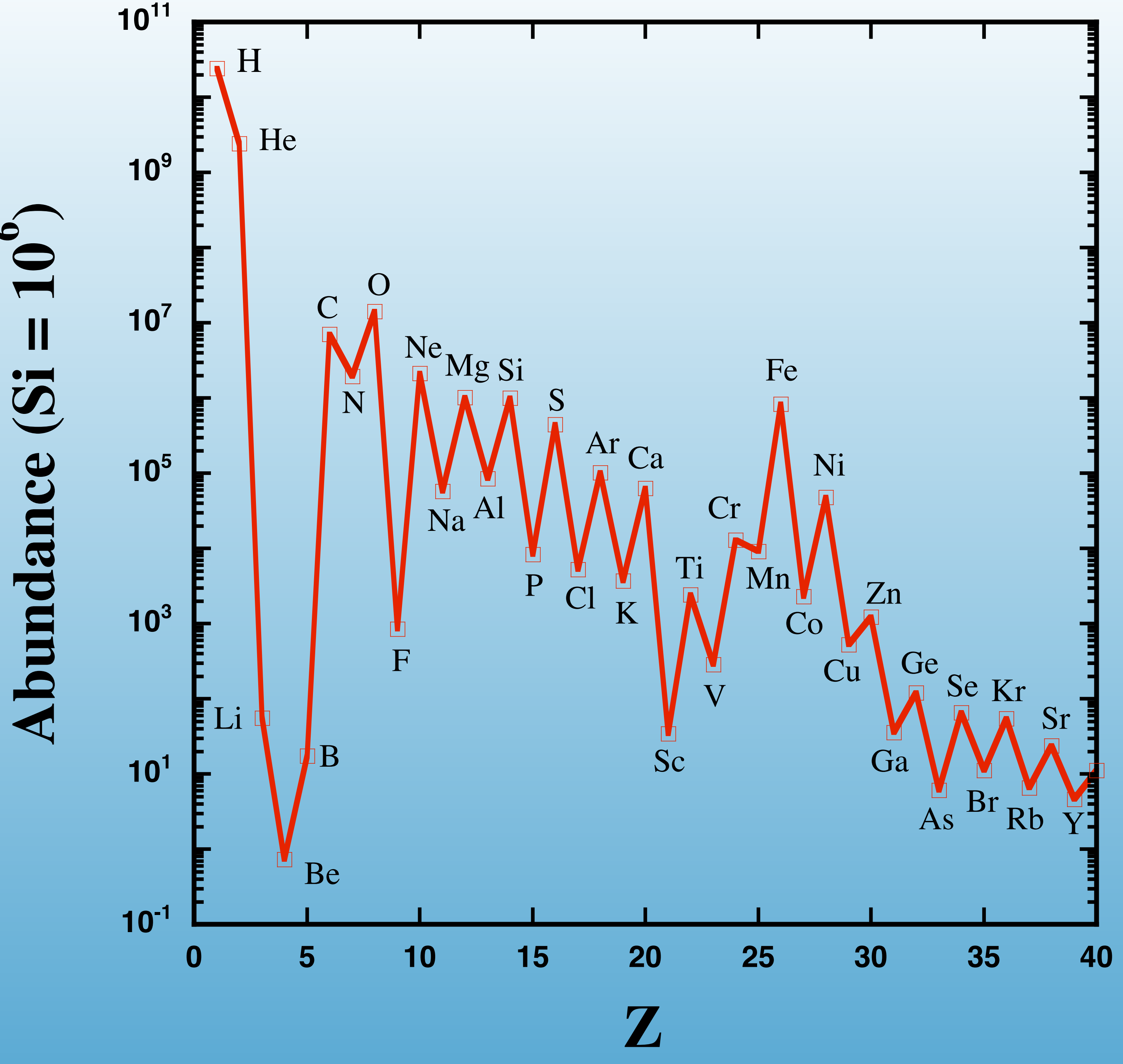

Abundance (Si = 10^6)
10^{11}
10^9
10^7
10^5
10^3
10^1
10^{-1}
H
He
Li
Be
B
C
N
O
F
Ne
Na
Mg
Al
Si
P
S
Cl
Ar
K
Ca
Sc
Ti
V
Cr
Mn
Fe
Co
Ni
Cu
Zn
Ga
Ge
As
Se
Br
Kr
Rb
Sr
Y
0
5
10
15
20
25
30
35
40
Z

Historical Perspective

Intimate connection with CMB

Alpher
Herman
Gamow

Conditions for BBN:

Require $T > 100$ keV $\Rightarrow t < 200$ s

$$\sigma v(p + n \rightarrow D + \gamma) \approx 5 \times 10^{-20}\ \mathrm{cm^3/s}$$

$$\Rightarrow n_B \sim 1/\sigma v t \sim 10^{17}\ \mathrm{cm^{-3}}$$

Today:

$$n_{Bo} \sim 10^{-7}\ \mathrm{cm^{-3}}$$

and

$$n_B \sim R^{-3} \sim T^3$$

Predicts the CMB temperature

$$T_o = (n_{Bo} / n_B)^{1/3}\, T_{BBN} \sim 10\ \mathrm{K}$$

Remarks on the Evolution of the Expanding Universe*, †

Ralph A. Alpher and Robert C. Herman
Applied Physics Laboratory, The Johns Hopkins University, Silver Spring, Maryland
(Received December 27, 1948)

Because of Eq. (4) a knowledge of $\rho_{m'}$ and $\rho_{r'}$ during the element forming period together with $\rho_{m''}$ fixes a value for $\rho_{r''}$, the present radiation density, which is perhaps the least well-known quantity.

In accordance with Eq. (4), the specification of $\rho_{m''}$, $\rho_{m'}$, and $\rho_{r'}$ fixes the present density of radiation, $\rho_{r''}$. In fact, we find that the value of $\rho_{r''}$ consistent with Eq. (4) is

$$\rho_{r''} \cong 10^{-32}\ \mathrm{g/cm^3}, \tag{12d}$$

which corresponds to a temperature now of the order of 5°K. This mean temperature for the universe is to be interpreted as the background temperature which would result from the universal expansion alone. However, the thermal energy resulting from the nuclear energy production in stars would increase this value.

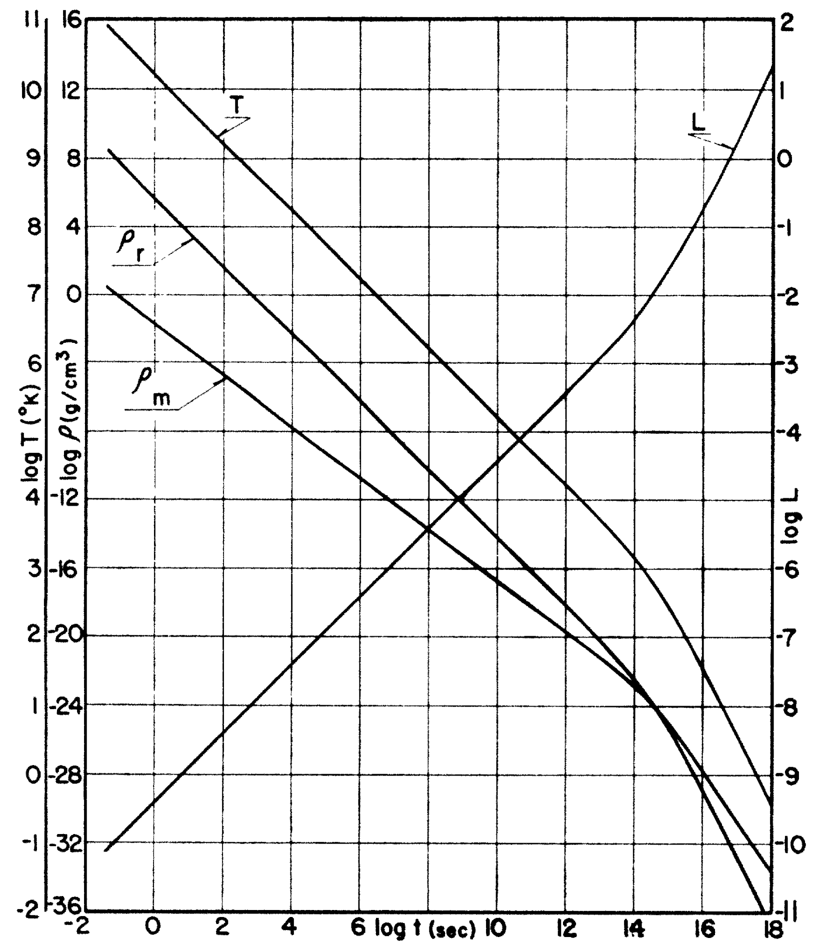

Fig. 1. The time dependence of the proper distance L, the densities of matter and radiation, ρ_m, and ρ_r, as well as the temperature, T, are shown for the case where $\rho_{m''} \cong 10^{-30}$ g/cm³, $\rho_{r''} \cong 10^{-32}$ g/cm³, $\rho_{m'} \cong 10^{-6}$ g/cm³, and $\rho_{r'} \cong 1$ g/cm³. [See Eq. (12).]

Remarks on the Evolution of the Expanding Universe*, †

RALPH A. ALPHER AND ROBERT C. HERMAN
Applied Physics Laboratory, The Johns Hopkins University, Silver Spring, Maryland

(Received December 27, 1948)

Because of Eq. (4) a knowledge of $\rho_{m'}$ and $\rho_{r'}$ during the element forming p
$\rho_{m''}$ fixes a value for $\rho_{r''}$, th
density, which is perhaps th
quantity.

In accordance with Eq. (4)
$\rho_{m''}$, $\rho_{m'}$, and $\rho_{r'}$ fixes the pres
tion, $\rho_{r''}$. In fact, we find tl
consistent with Eq. (4) is

$$\rho_{r''} \cong 10^{-32} \text{ g/cm}^3, \qquad (12d)$$

which corresponds to a temperature now of the order of 5°K. This mean temperature for the universe is to be interpreted as the background temperature which would result from the universal expansion alone. However, the thermal energy resulting from the nuclear energy production in stars would increase this value.

In order to study how sensitive this model is to the choice of densities, we have considered the following additional set of density values which satisfy Eq. (4):

$$\begin{aligned} \rho_{m'} &\cong 1.78 \times 10^{-4} \text{ g/cm}^3, \\ \rho_{r'} &\cong 1 \text{ g/cm}^3, \qquad (15) \\ \rho_{m''} &\cong 10^{-30} \text{ g/cm}^3, \end{aligned}$$

and

$$\rho_{r''} \cong 10^{-35} \text{ g/cm}^3.$$

The value obtained for $\rho_{r''}$ in this case corresponds to a present mean temperature of about 1°K. The

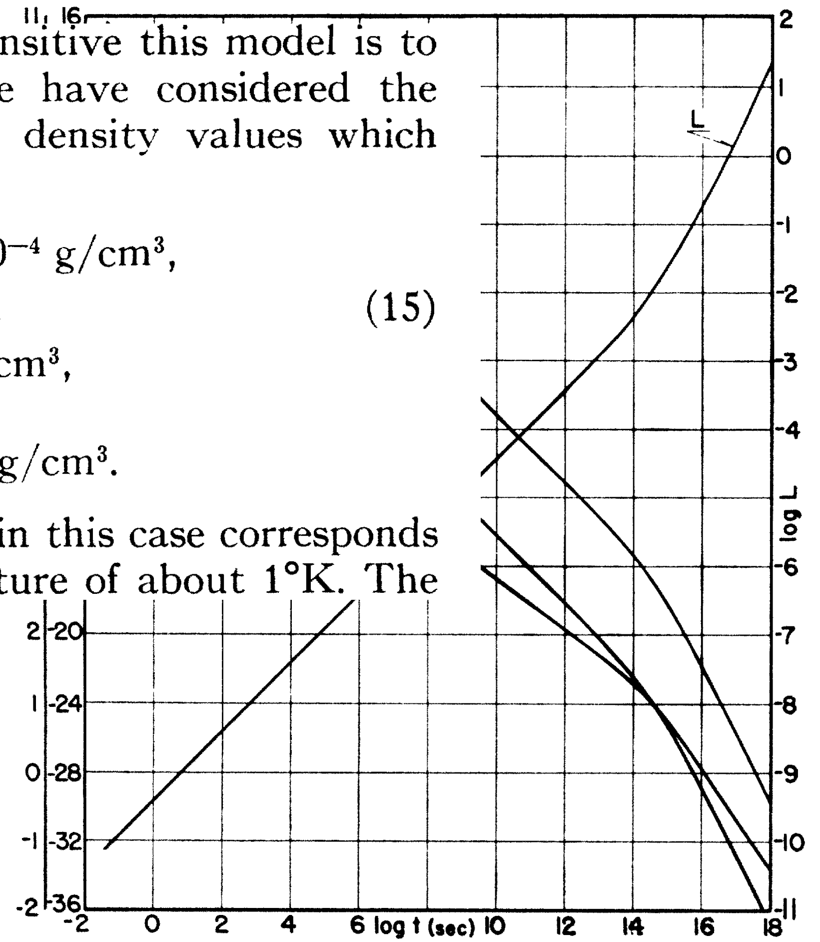

FIG. 1. The time dependence of the proper distance L, the densities of matter and radiation, ρ_m, and ρ_r, as well as the temperature, T, are shown for the case where $\rho_{m''} \cong 10^{-30}$ g/cm³, $\rho_{r''} \cong 10^{-32}$ g/cm³, $\rho_{m'} \cong 10^{-6}$ g/cm³, and $\rho_{r'} \cong 1$ g/cm³. [See Eq. (12).]

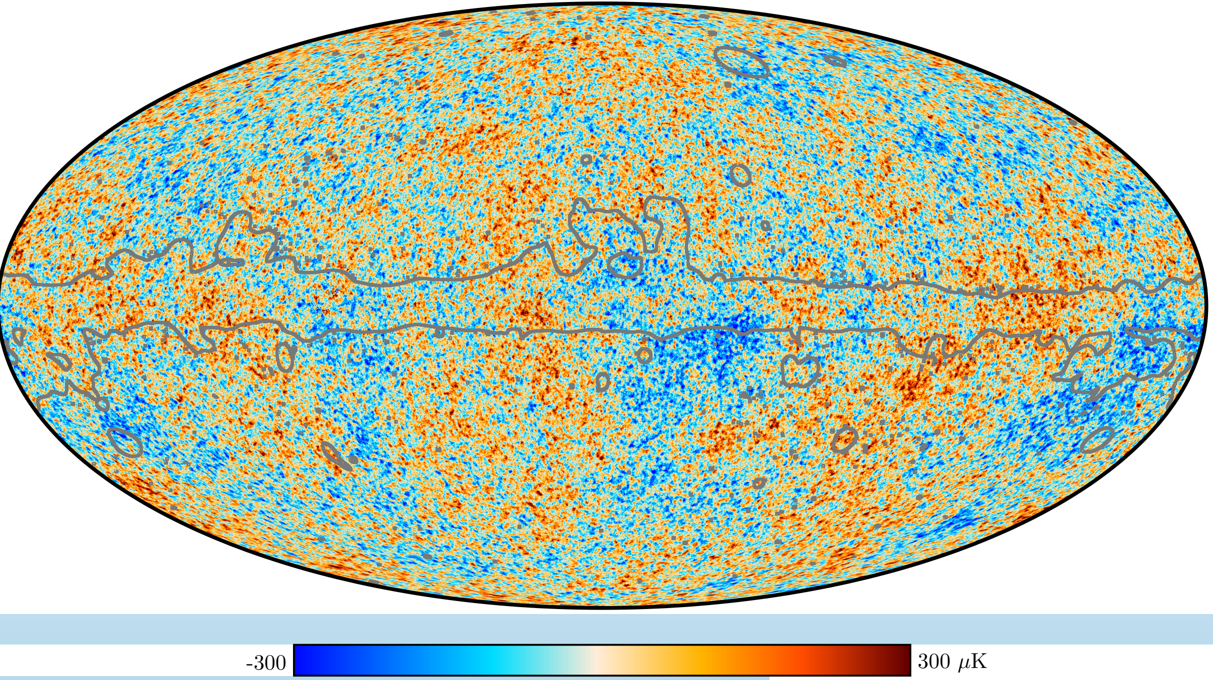

Planck best fit

$\Omega_B h^2 = 0.02237 \pm 0.00015$

$\eta_{10} = 6.12 \pm 0.04$

T = 2.7255±0.0006 K

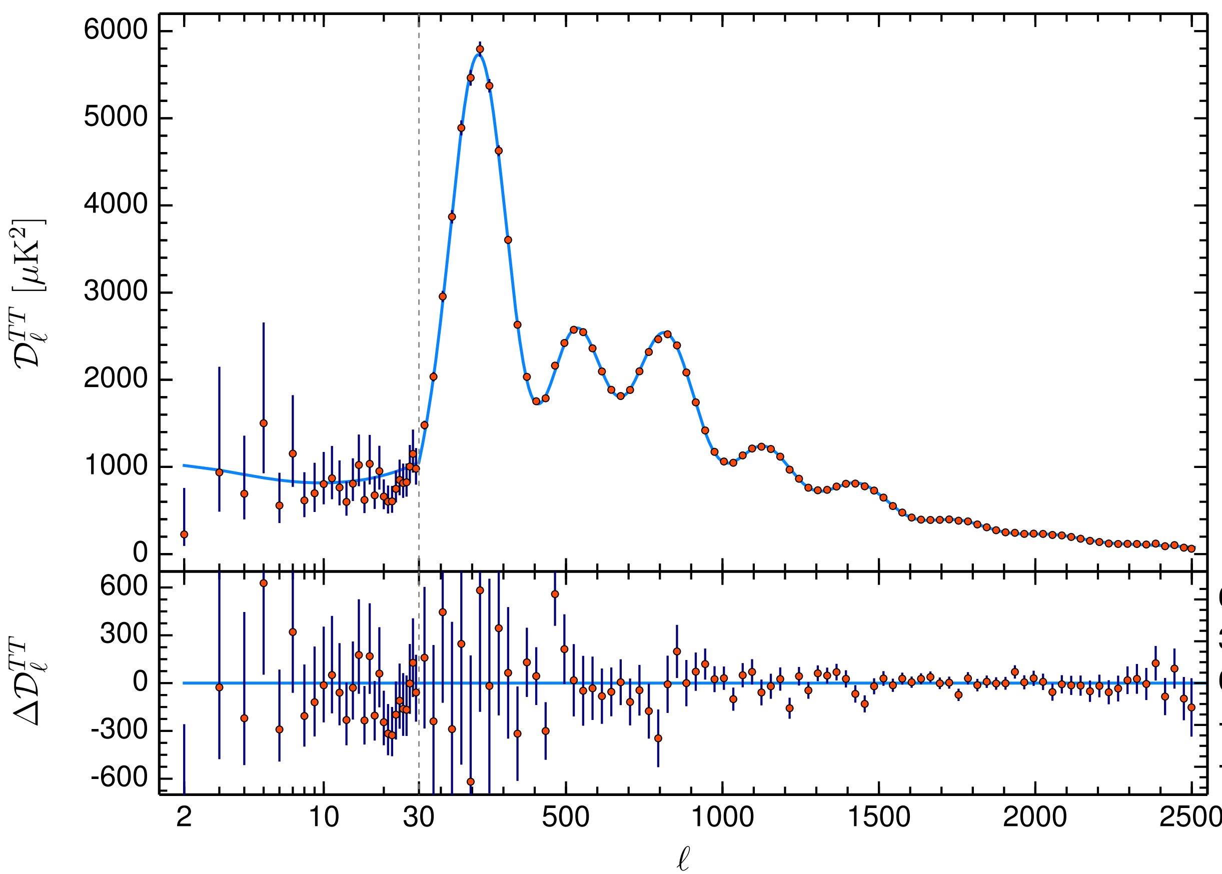

Conditions in the Early Universe:

$$T \gtrsim 1 \ \mathbf{MeV}$$

$$\rho = \frac{\pi^2}{30}(2 + \frac{7}{2} + \frac{7}{4}N_\nu)T^4$$

$$\eta = n_B/n_\gamma \sim 10^{-10}$$

β-Equilibrium maintained by weak interactions

Freeze-out at ~ 1 MeV determined by the competition of expansion rate $H \sim T^2/M_p$ and the weak interaction rate $\Gamma \sim G_F^2 T^5$

$$\begin{aligned} n + e^+ &\leftrightarrow p + \bar{\nu}_e \\ n + \nu_e &\leftrightarrow p + e^- \\ n &\leftrightarrow p + e^- + \bar{\nu}_e \end{aligned}$$

At freezeout n/p fixed modulo free neutron decay, $(n/p) \simeq 1/6 \rightarrow 1/7$

Nucleosynthesis Delayed (Deuterium Bottleneck)

$$p + n \rightarrow \mathbf{D} + \gamma \qquad \Gamma_p \sim n_B \sigma$$

$$p + n \leftarrow \mathbf{D} + \gamma \qquad \Gamma_d \sim n_\gamma \sigma e^{-E_B/T}$$

Nucleosynthesis begins when $\Gamma_p \sim \Gamma_d$

$$\frac{n_\gamma}{n_B} e^{-E_B/T} \sim 1 \qquad \text{@ } T \sim 0.1 \text{ MeV}$$

All neutrons $\rightarrow$ ^{4}**He**

$$Y_p = \frac{2(n/p)}{1 + (n/p)} \simeq 25\%$$

Remainder:

D, ^{3}**He** $\sim 10^{-5}$ **and** ^{7}**Li** $\sim 10^{-10}$ **by number**

BBN could <u>not</u> explain the abundances (or patterns) of <u>all</u> the elements.

$\Longrightarrow$ growth of stellar nucleosynthesis

But,

Questions persisted:

25% (by mass) of ^{4}He ?

D?

Resurgence:

BBN could successfully account for the abundance of

D, ^{3}He, ^{4}He, ^{7}Li.

1	2	3	4	5	6	7	8	9	10	11	12	13	14	15	16	17	18
1 H 1.008																	2 He 4.0026
3 Li 6.94	4 Be 9.0122											5 B 10.81	6 C 12.011	7 N 14.007	8 O 15.999	9 F 18.998	10 Ne 20.180
11 Na 22.990	12 Mg 24.305											13 Al 26.982	14 Si 28.085	15 P 30.974	16 S 32.06	17 Cl 35.45	18 Ar 39.948
19 K 39.098	20 Ca 40.078	21 Sc 44.956	22 Ti 47.867	23 V 50.942	24 Cr 51.996	25 Mn 54.938	26 Fe 55.845	27 Co 58.933	28 Ni 58.693	29 Cu 63.546	30 Zn 65.38	31 Ga 69.723	32 Ge 72.630	33 As 74.922	34 Se 78.971	35 Br 79.904	36 Kr 83.798
37 Rb 85.468	38 Sr 87.62	39 Y 88.906	40 Zr 91.224	41 Nb 92.906	42 Mo 95.95	43 Tc 96.906	44 Ru 101.07	45 Rh 102.91	46 Pd 106.42	47 Ag 107.87	48 Cd 112.41	49 In 114.82	50 Sn 118.71	51 Sb 121.76	52 Te 127.60	53 I 126.90	54 Xe 131.29
55 Cs 132.91	56 Ba 137.33	71 Lu 174.97	72 Hf 178.49	73 Ta 180.95	74 W 183.84	75 Re 186.21	76 Os 190.23	77 Ir 192.22	78 Pt 195.08	79 Au 196.97	80 Hg 200.59	81 Tl 204.38	82 Pb 207.2	83 Bi 208.98	84 Po 208.98	85 At 209.99	86 Rn 222.02
87 Fr 223.02	88 Ra 226.03	103 Lr 262.11	104 Rf 267.12	105 Db 270.13	106 Sg 269.13	107 Bh 270.13	108 Hs 269.13	109 Mt 278.16	110 Ds 281.17	111 Rg 281.17	112 Cn 285.18	113 Nh 286.18	114 Fl 289.19	115 Mc 289.20	116 Lv 293.20	117 Ts 293.21	118 Og 294.21

		57 La 138.91	58 Ce 140.12	59 Pr 140.91	60 Nd 144.24	61 Pm 144.91	62 Sm 150.36	63 Eu 151.96	64 Gd 157.25	65 Tb 158.93	66 Dy 162.50	67 Ho 164.93	68 Er 167.26	69 Tm 168.93	70 Yb 173.05		
		89 Ac 227.03	90 Th 232.04	91 Pa 231.04	92 U 238.03	93 Np 237.05	94 Pu 244.06	95 Am 243.06	96 Cm 247.07	97 Bk 247.07	98 Cf 251.08	99 Es 252.08	100 Fm 257.10	101 Md 258.10	102 No 259.10		

Periodic Table

www.webelements.com

η vs Ω_B h^2

baryon density

$$\rho_B = m_N n_N = \Omega_B \rho_c \left(\frac{T}{T_0}\right)^3$$

then

$$\eta = \frac{n_B}{n_\gamma} = \Omega_B \frac{\rho_c}{m_N n_\gamma}$$

$$\rho_c = 1.05 \times 10^{-5} h^2 \mathrm{GeV/cm}^3$$

$$n_\gamma = 411 \mathrm{cm}^{-3}$$

$$\eta = 2.73 \times 10^{-8} \Omega_B h^2$$

$$\Omega_B h^2 = 3.66 \times 10^7 \eta$$

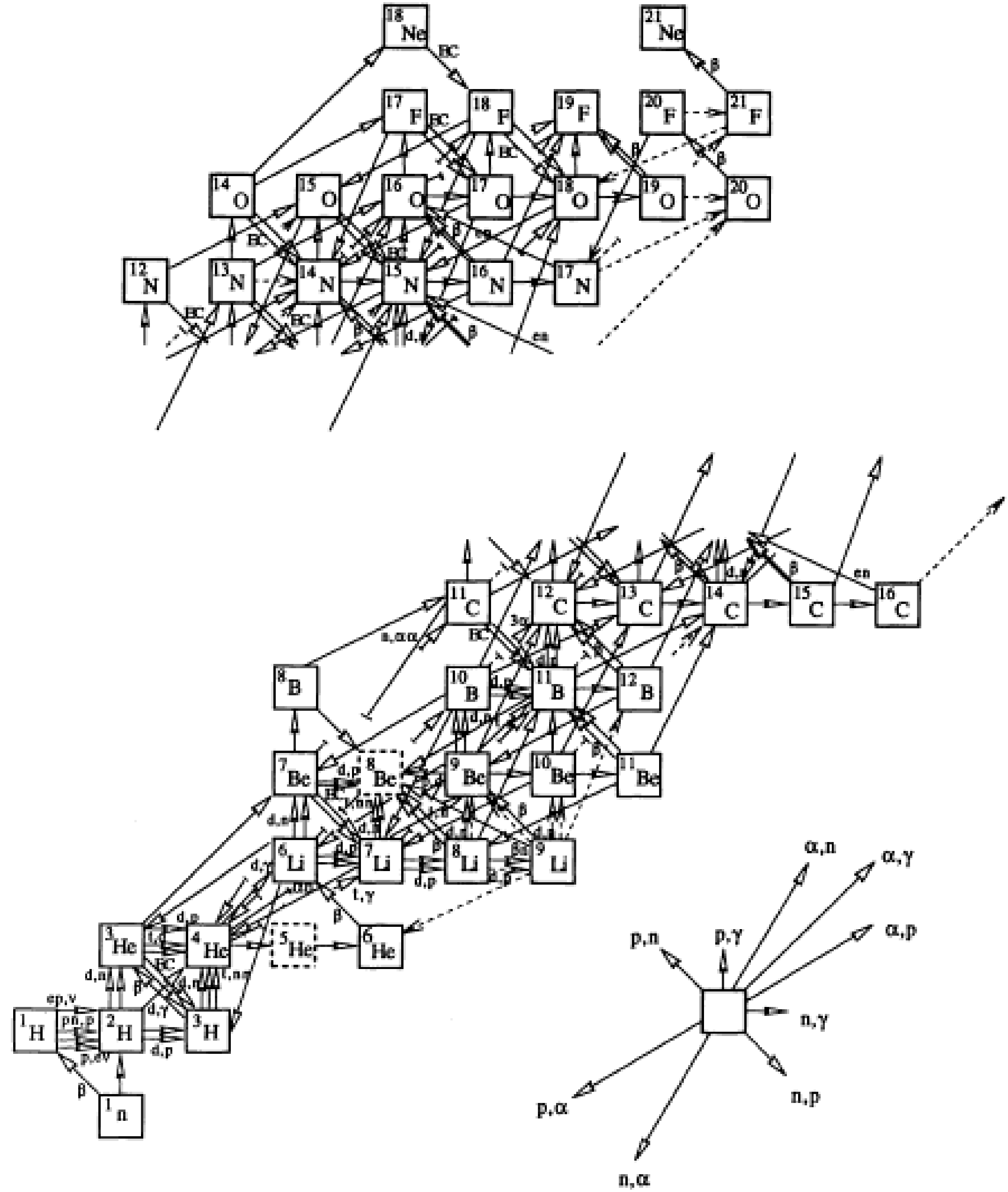

FIG. 1.—Reaction network used in the code. Estimated reactions are shown with dashed lines.

Table 1: Key Nuclear Reactions for BBN

Source	Reactions	
NACRE	$d(p,\gamma)^3$He	(b)
	$d(d,n)^3$He	
	$d(d,p)t$	
	$t(d,n)^4$He	
	$t(\alpha,\gamma)^7$Li	(d)
	^{3}He$(\alpha,\gamma)^7$Be	(c)
	^{7}Li$(p,\alpha)^4$He	
SKM	$p(n,\gamma)d$	
	^{3}He$(d,p)^4$He	
	^{7}Be$(n,p)^7$Li	(See below)
This work	^{3}He$(n,p)t$	(a)
PDG	τ_n	

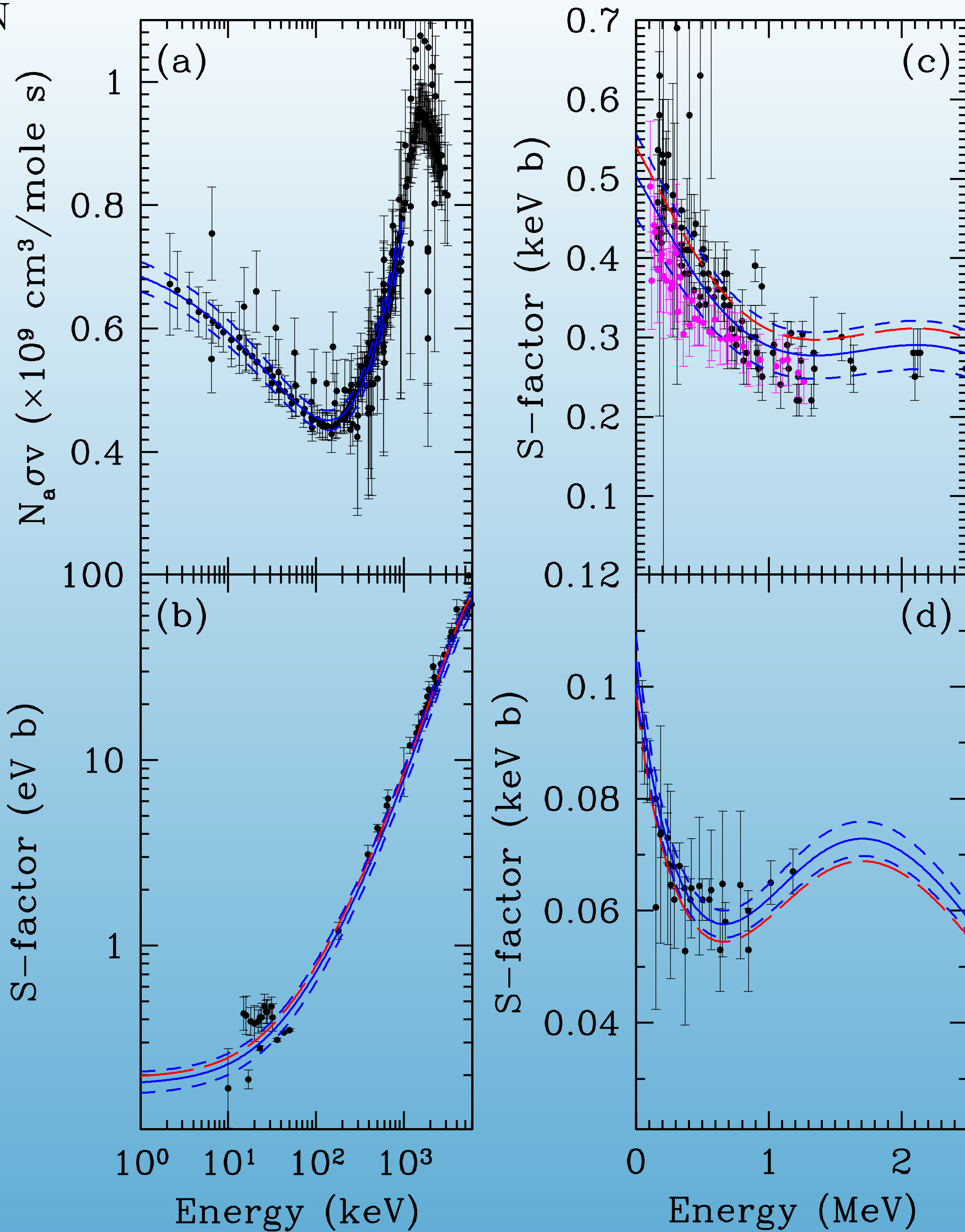

NACRE
Cyburt, Fields, KAO
Nollett & Burles
Coc et al.

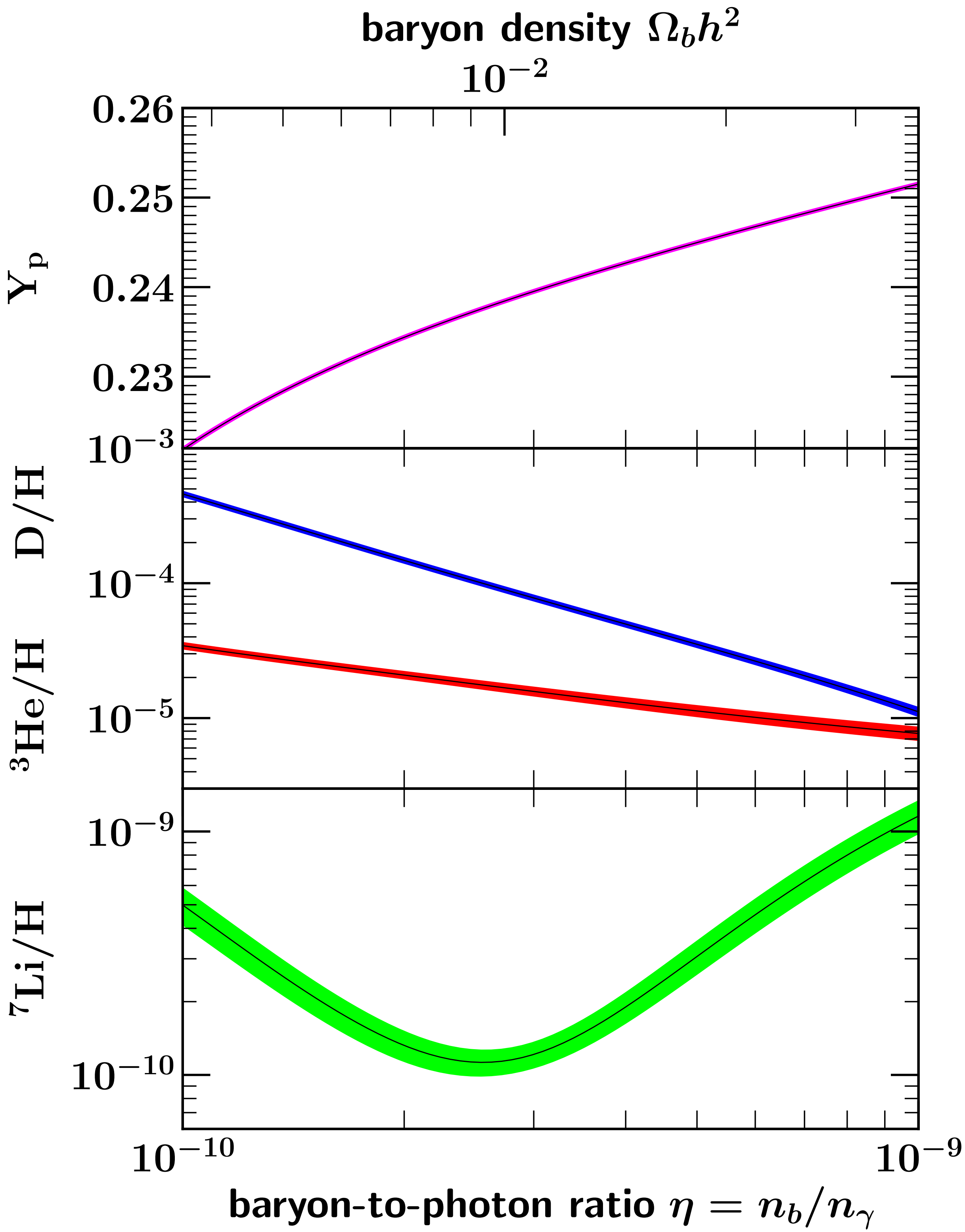

Fields, Olive, Yeh, Young

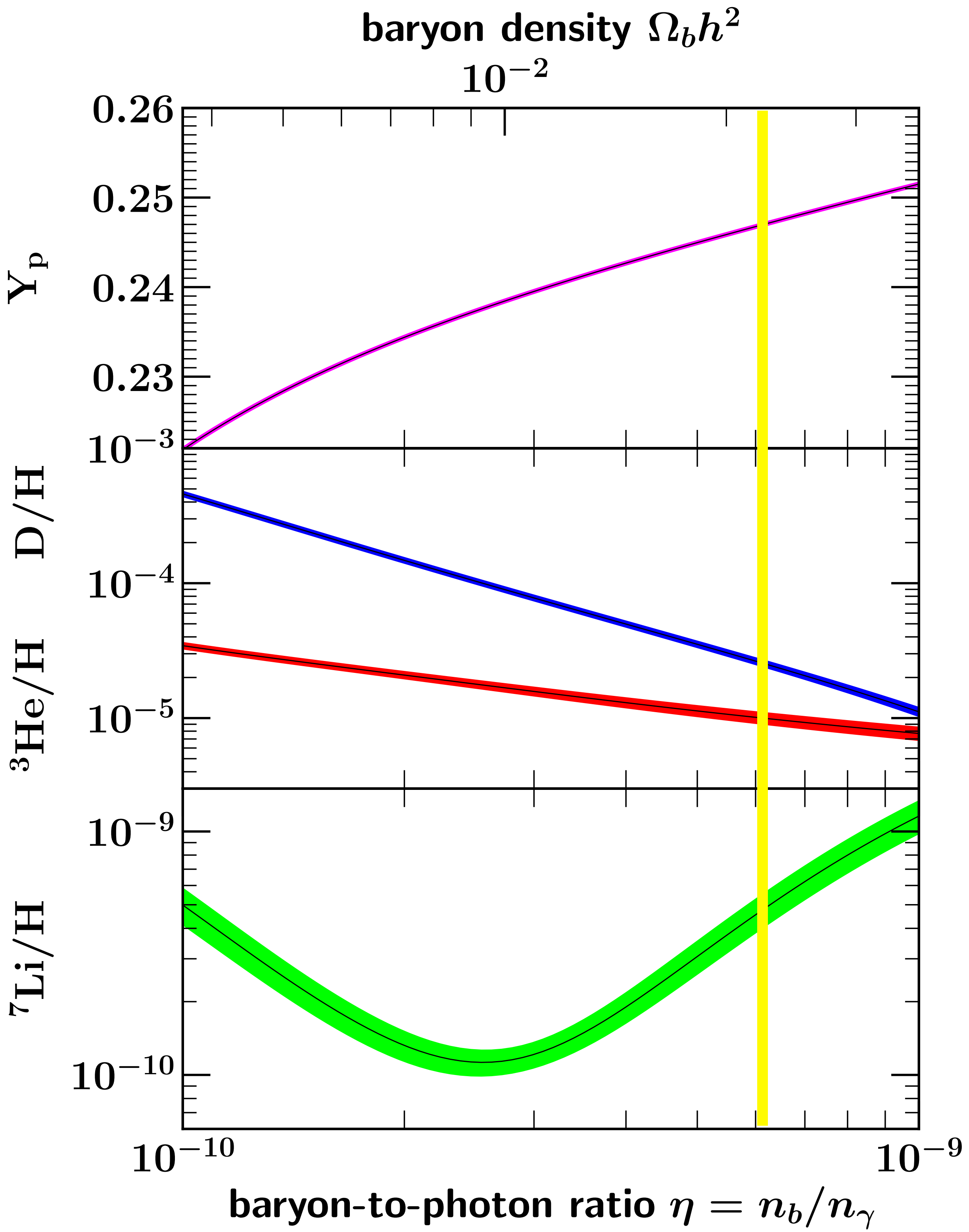

Fields, Olive, Yeh, Young

Observations

- Production of the Light Elements: D, ^{3}He, ^{4}He, ^{7}Li
  - ^{4}He observed in extragalctic HII regions:
    abundance by mass = 25%
  - ^{7}Li observed in the atmospheres of dwarf halo stars:
    abundance by number = 10^{-10}
  - D observed in quasar absorption systems (and locally):
    abundance by number = 3×10^{-5}
  - ^{3}He in solar wind, in meteorites, and in the ISM:
    abundance by number = 10^{-5}

D/H

- All Observed D is Primordial!
- Observed in the ISM and inferred from meteoritic samples (also HD in Jupiter)
- D/H observed in Quasar Absorption systems

Table 3. PRECISION D/H MEASURES CONSIDERED IN THIS PAPER

QSO	z_{em}	z_{abs}	$\log_{10} N(\mathrm{H\,I})/\mathrm{cm}^{-2}$	[O/H][a]	$\log_{10} N(\mathrm{D\,I})/N(\mathrm{H\,I})$
HS 0105+1619	2.652	2.53651	19.426 ± 0.006	-1.771 ± 0.021	-4.589 ± 0.026
Q0913+072	2.785	2.61829	20.312 ± 0.008	-2.416 ± 0.011	-4.597 ± 0.018
Q1243+307	2.558	2.52564	19.761 ± 0.026	-2.769 ± 0.028	-4.622 ± 0.015
SDSS J1358+0349	2.894	2.85305	20.524 ± 0.006	-2.804 ± 0.015	-4.582 ± 0.012
SDSS J1358+6522	3.173	3.06726	20.495 ± 0.008	-2.335 ± 0.022	-4.588 ± 0.012
SDSS J1419+0829	3.030	3.04973	20.392 ± 0.003	-1.922 ± 0.010	-4.601 ± 0.009
SDSS J1558−0031	2.823	2.70242	20.75 ± 0.03	-1.650 ± 0.040	-4.619 ± 0.026

[a]We adopt the solar value $\log_{10}(\mathrm{O/H}) + 12 = 8.69$ (Asplund et al. 2009).

Cooke et al.

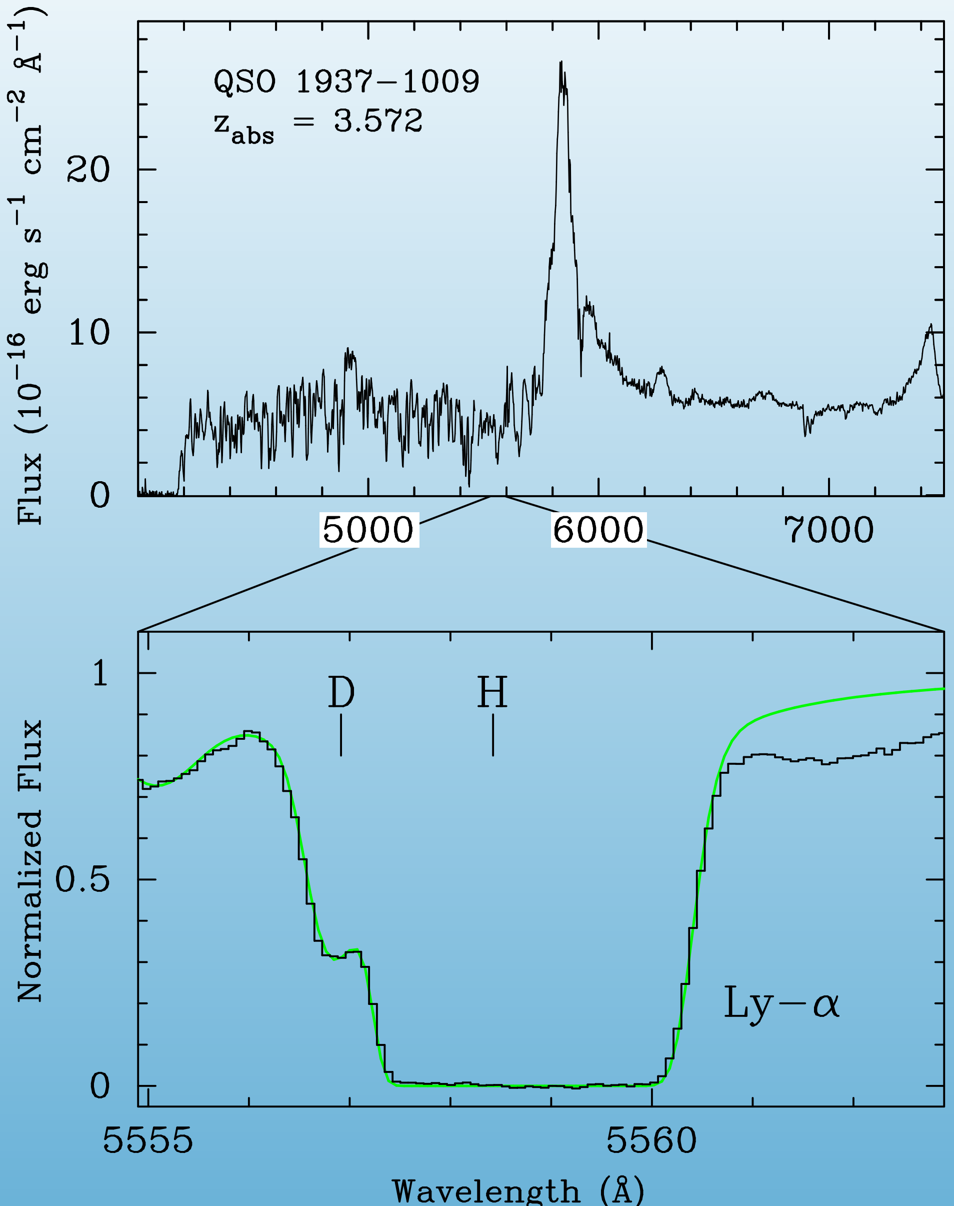

Tytler, O’Meara, Suzuki, Lubin

Updated
D/H abundances in
Quasar absorption
systems

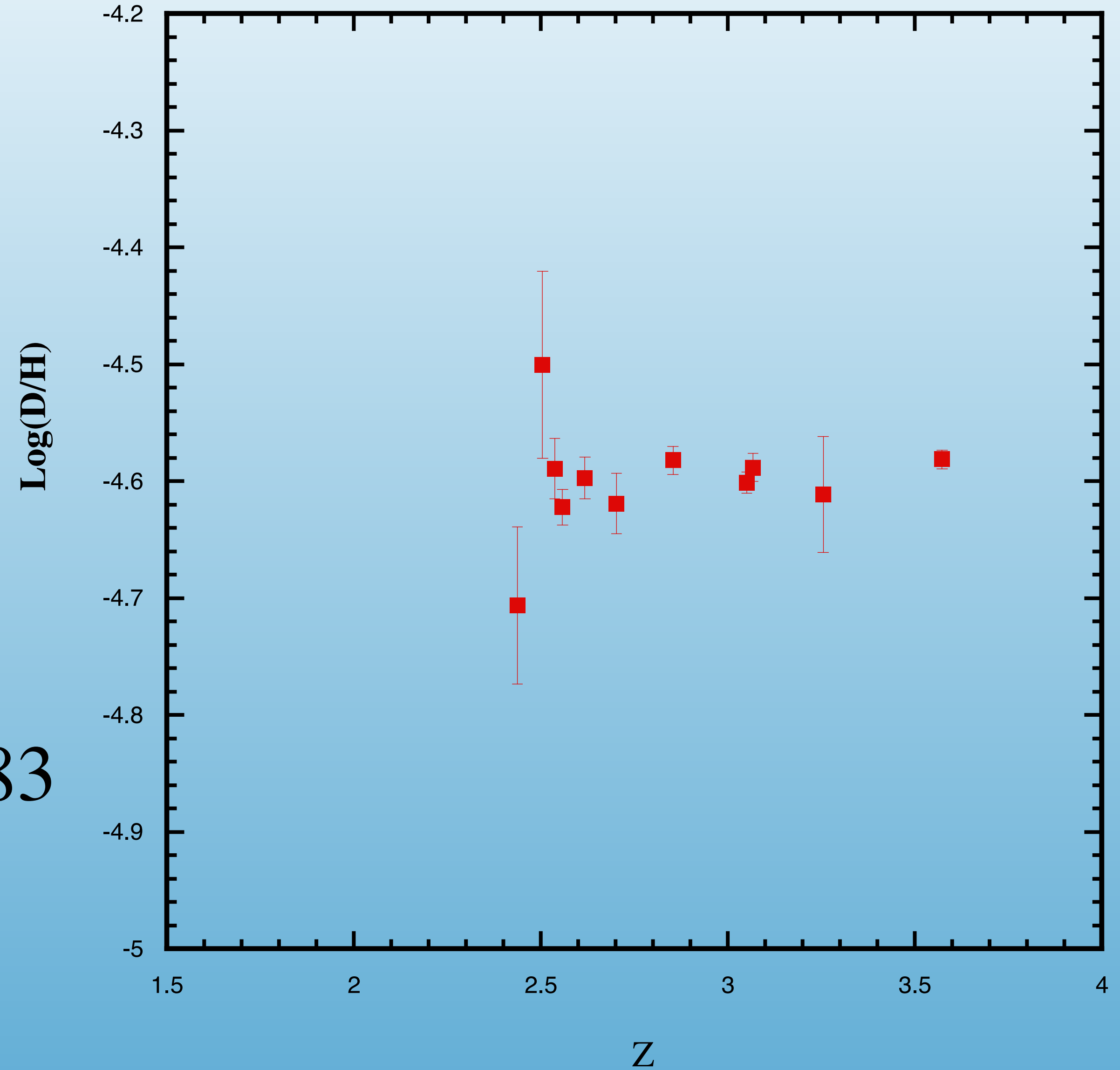

BBN Prediction:
10^5 D/H = 2.506 ± 0.083

Obs Average:
10^5 D/H = 2.55 ± 0.03

Updated D/H abundances in Quasar absorption systems

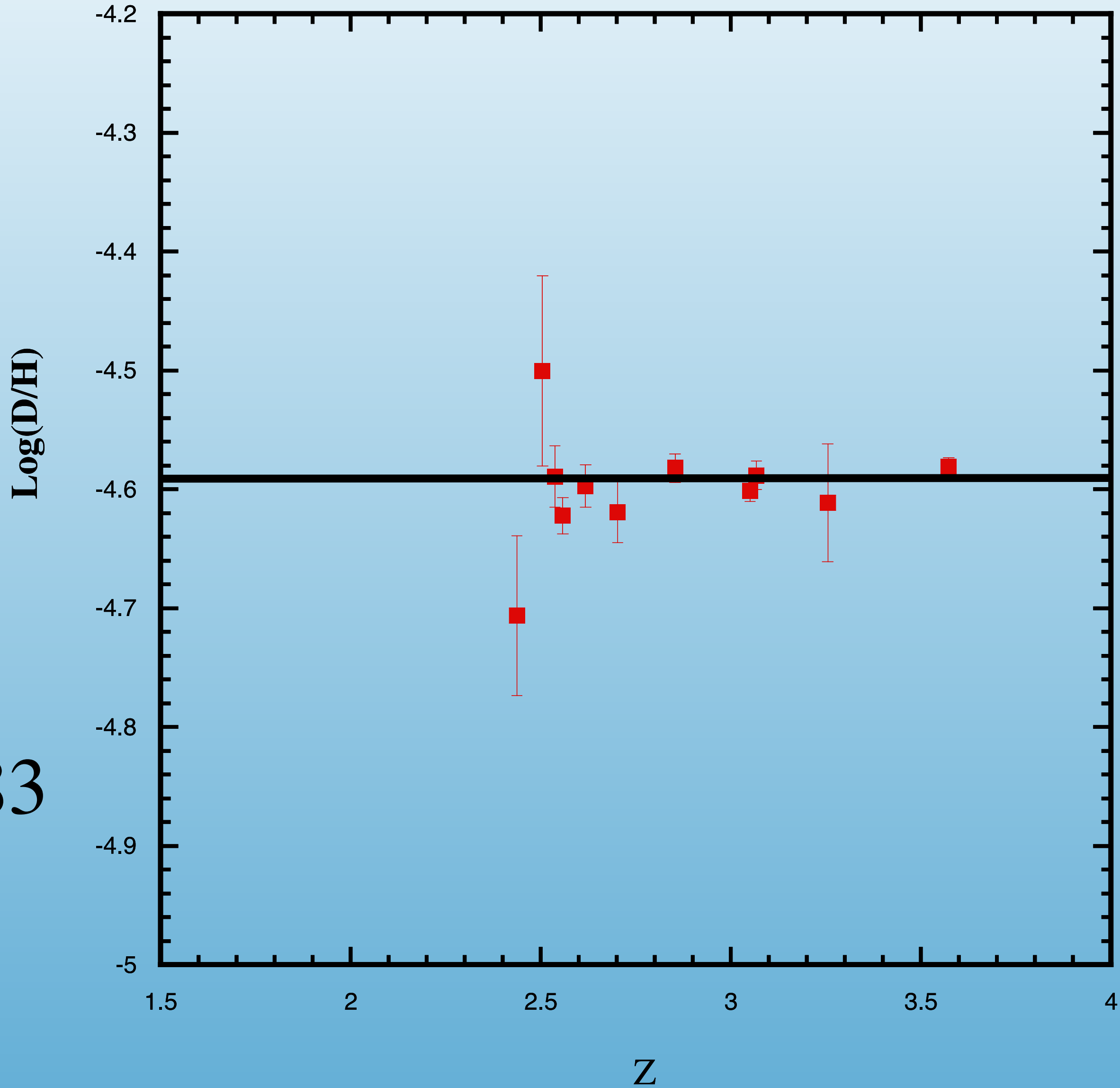

BBN Prediction:

10^5 D/H = 2.506 ± 0.083

Obs Average:

10^5 D/H = 2.55 ± 0.03

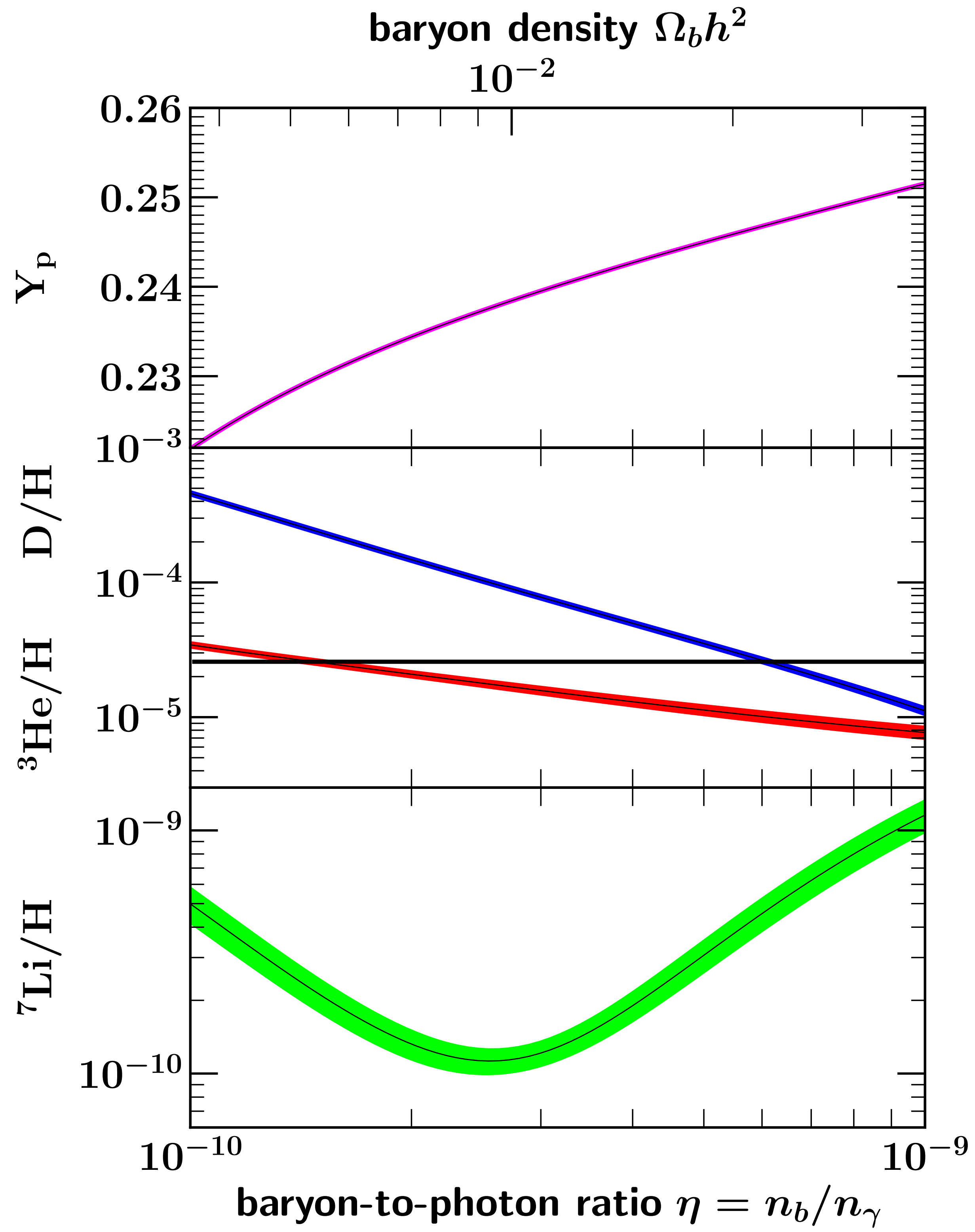

Fields, Olive, Yeh, Young

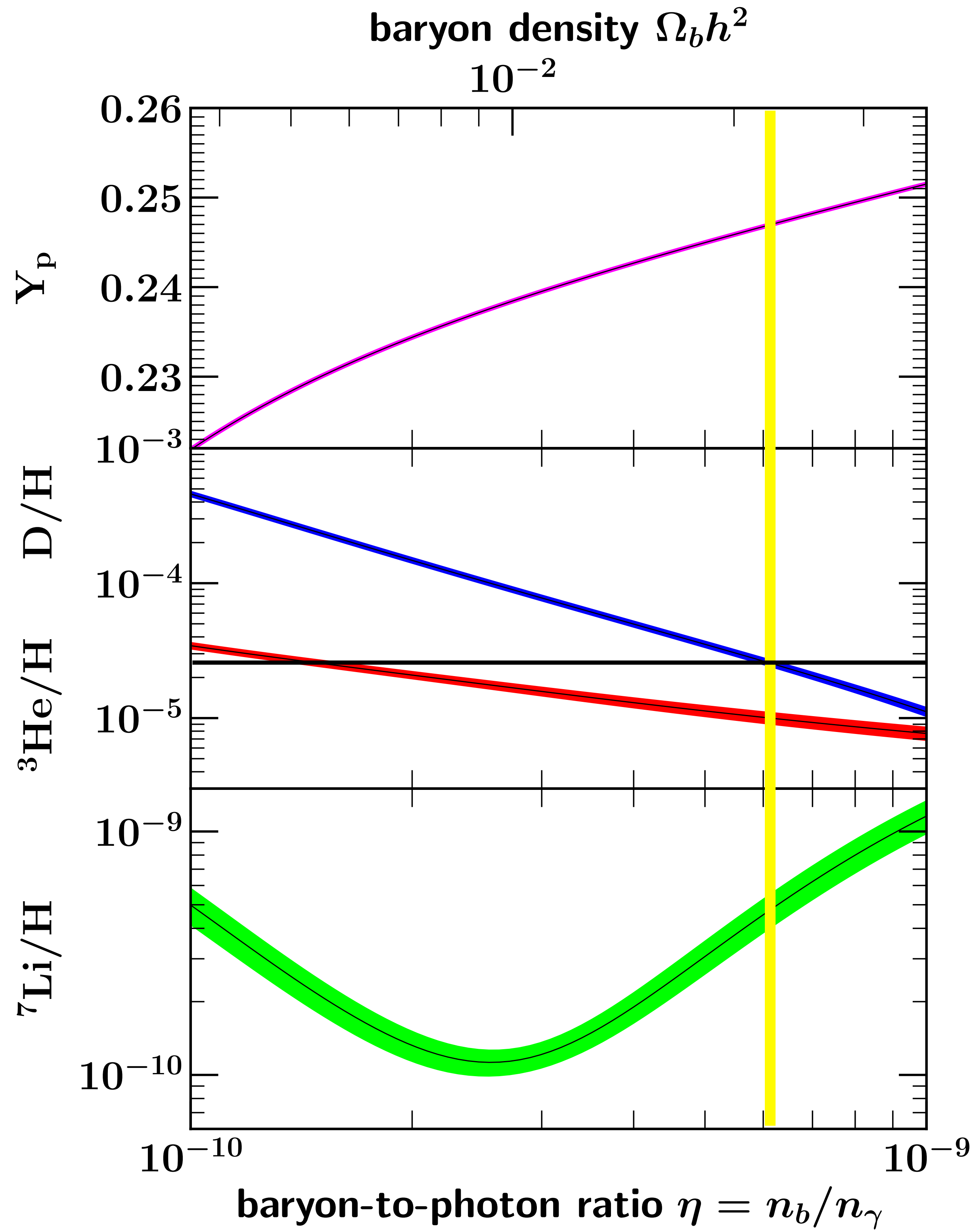

Fields, Olive, Yeh, Young

^{4}He

Measured in low metallicity extragalactic HII regions (~100) together with O/H and N/H

$$Y_P = Y(O/H \rightarrow 0)$$

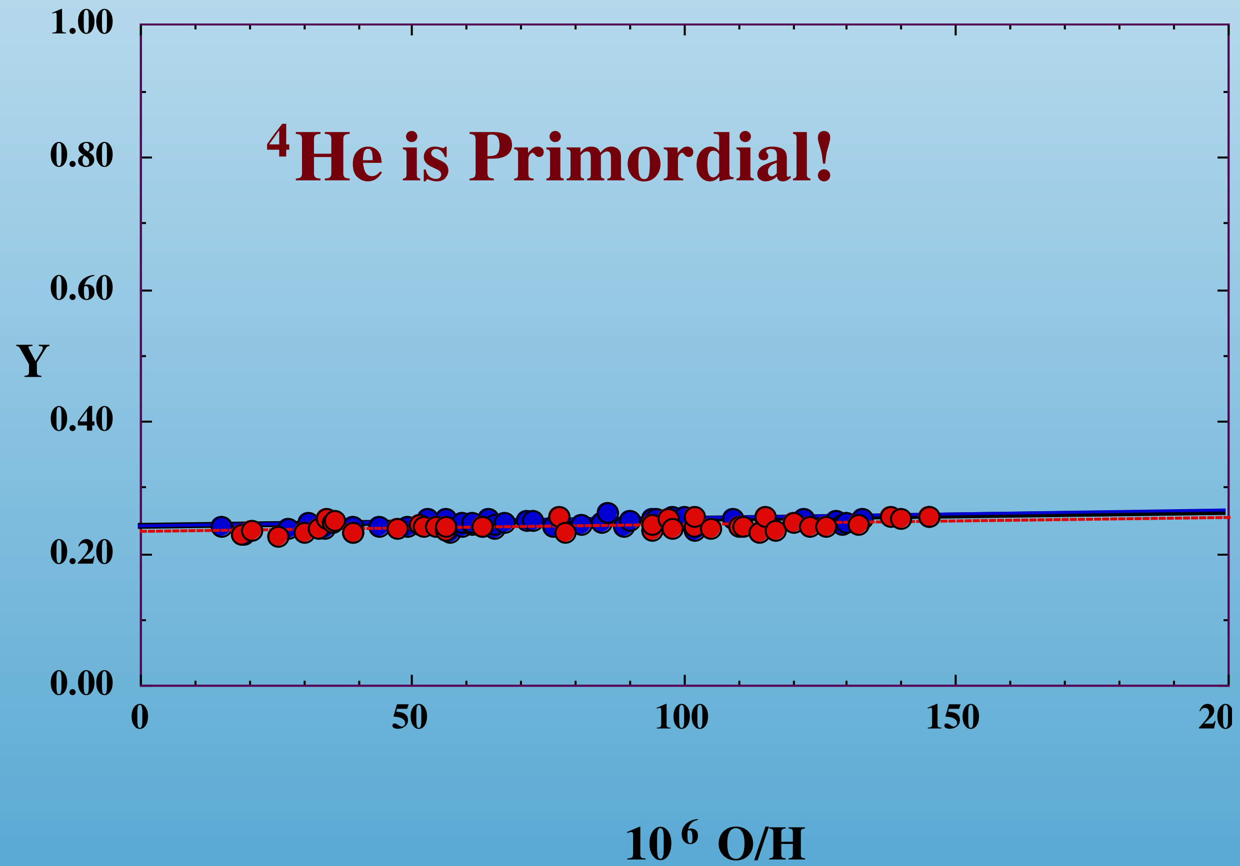

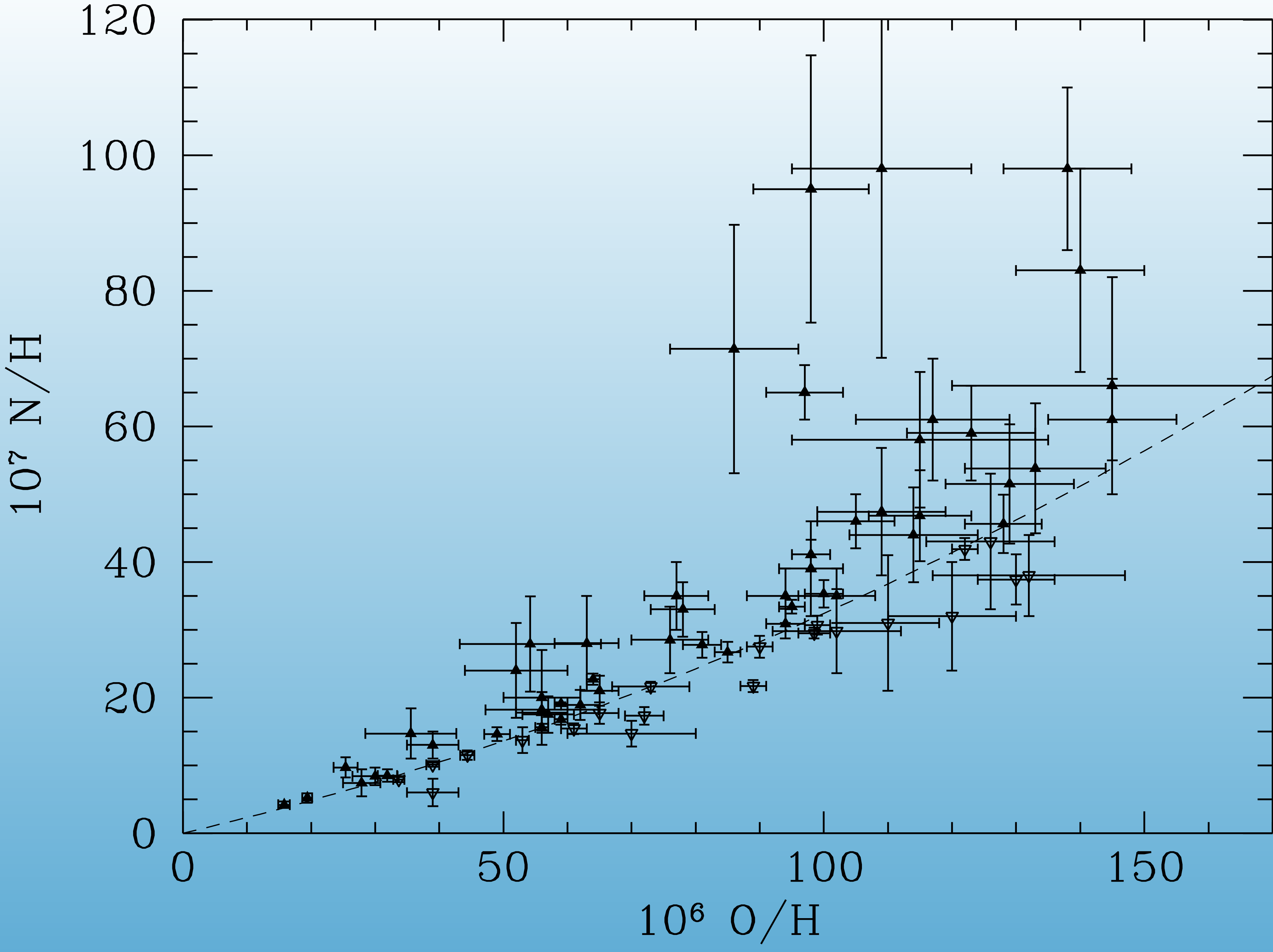

120
100
80
60
40
20
0
0
50
100
150
10⁷ N/H
10⁶ O/H

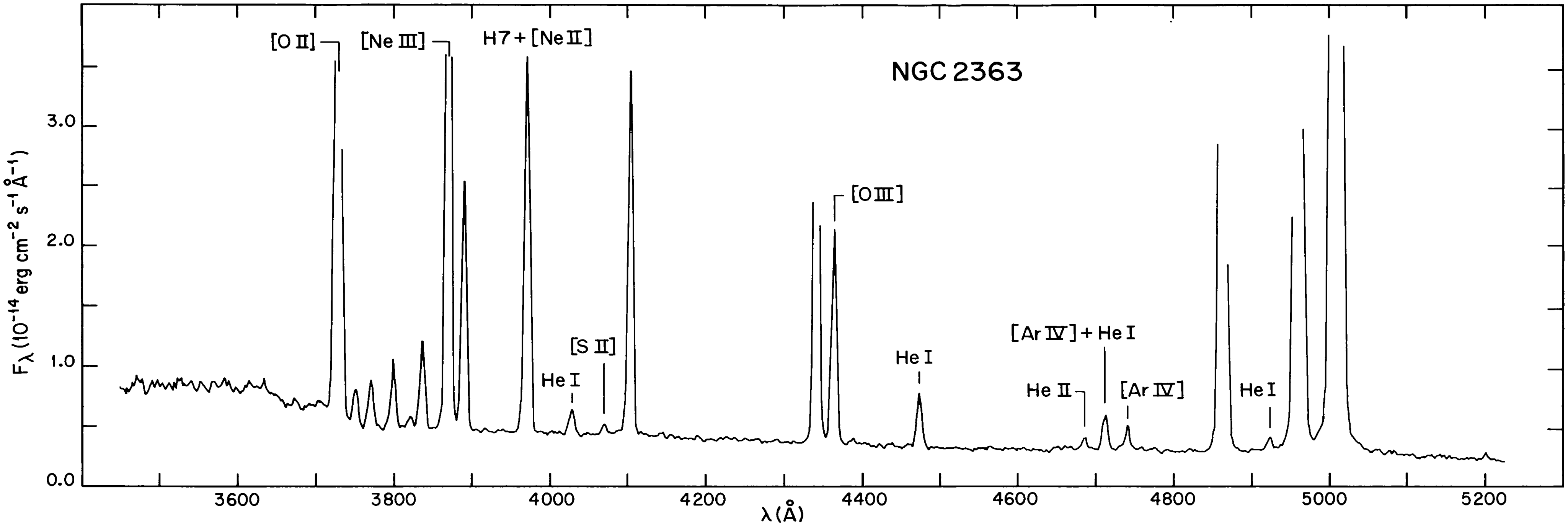

Fig. 1. Low dispersion blue spectrogram of NGC 2363, showing the faintest lines measured

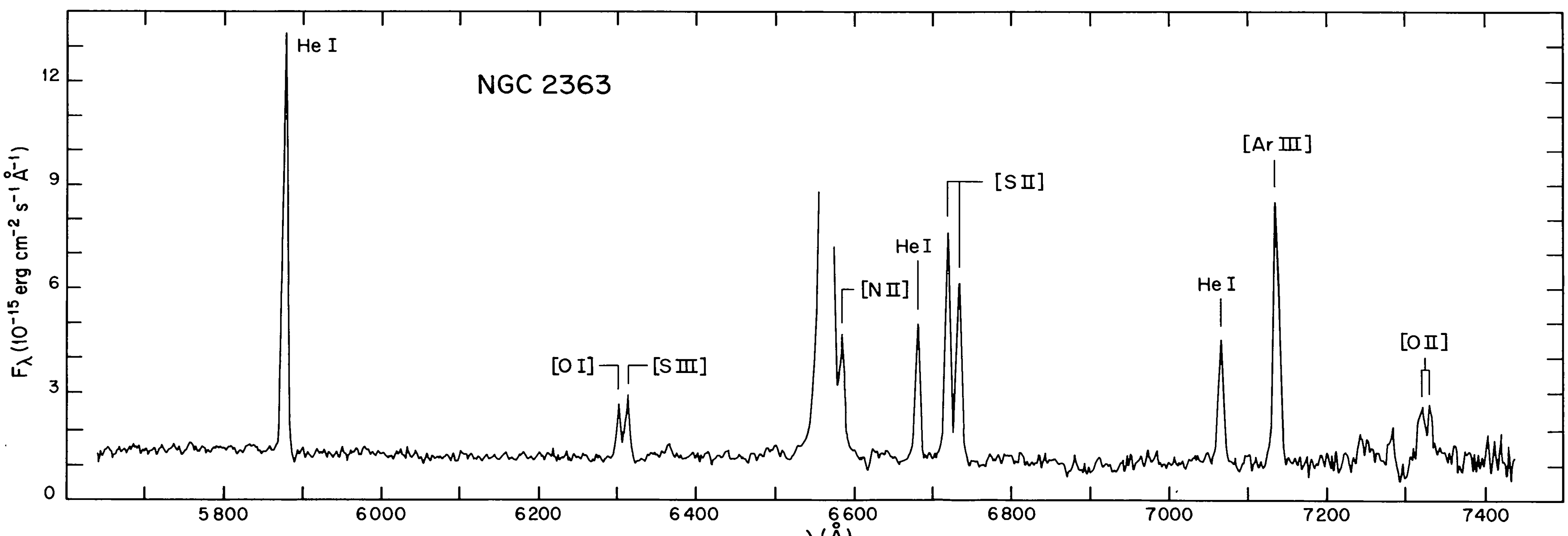

Fig. 2. Low dispersion red spectrogram of NGC 2363

Most recent addition: AGC 198691 (2021)

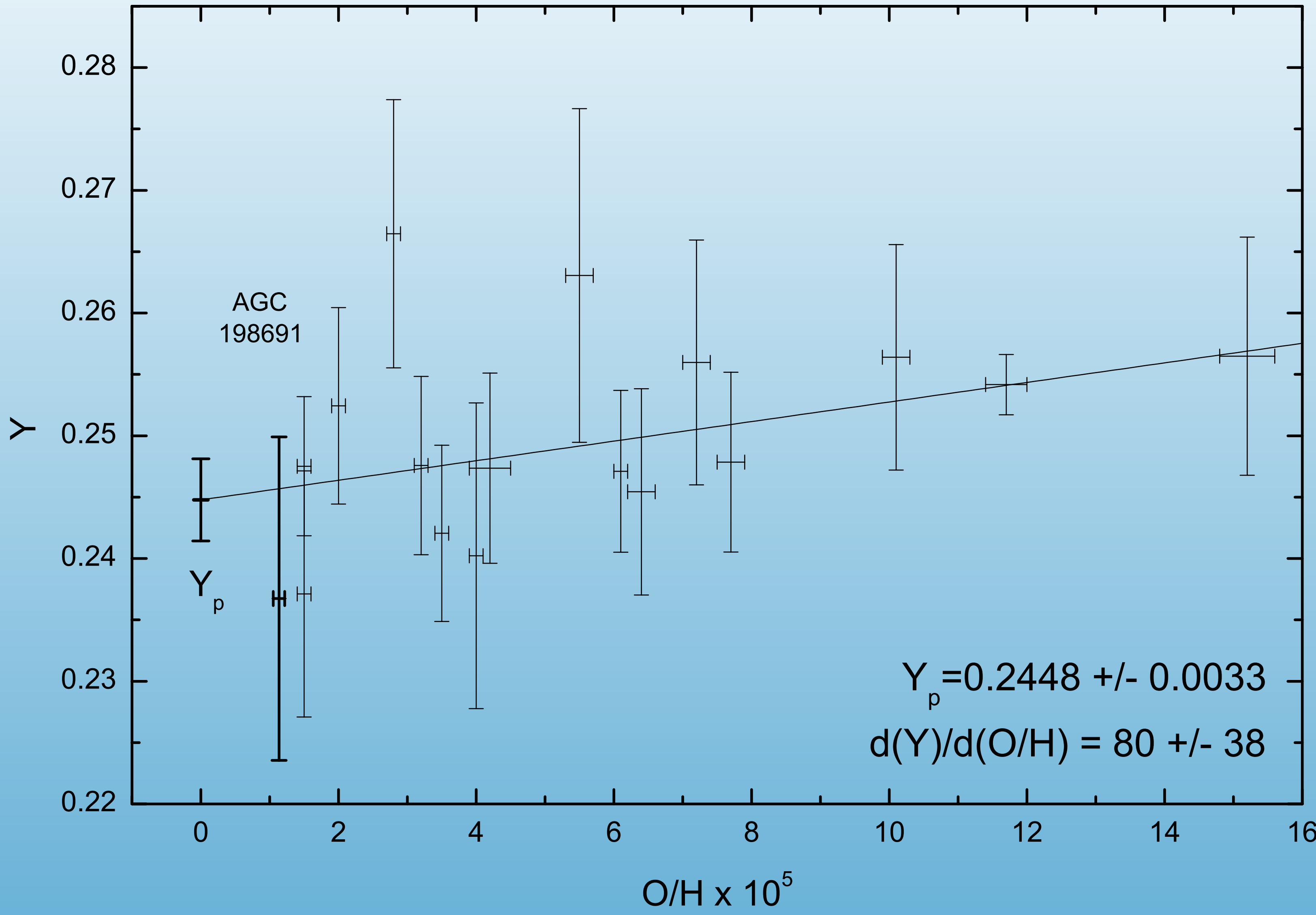

Aver, Berg, Hirschauer, Olive, Pogge, Rogers, Salzer, Skillman

prior: Y_P = .2453 ± 0.0034

^{4}He Prediction:
0.2467 ± 0.0002

Data: Regression:
0.2448 ± 0.0033

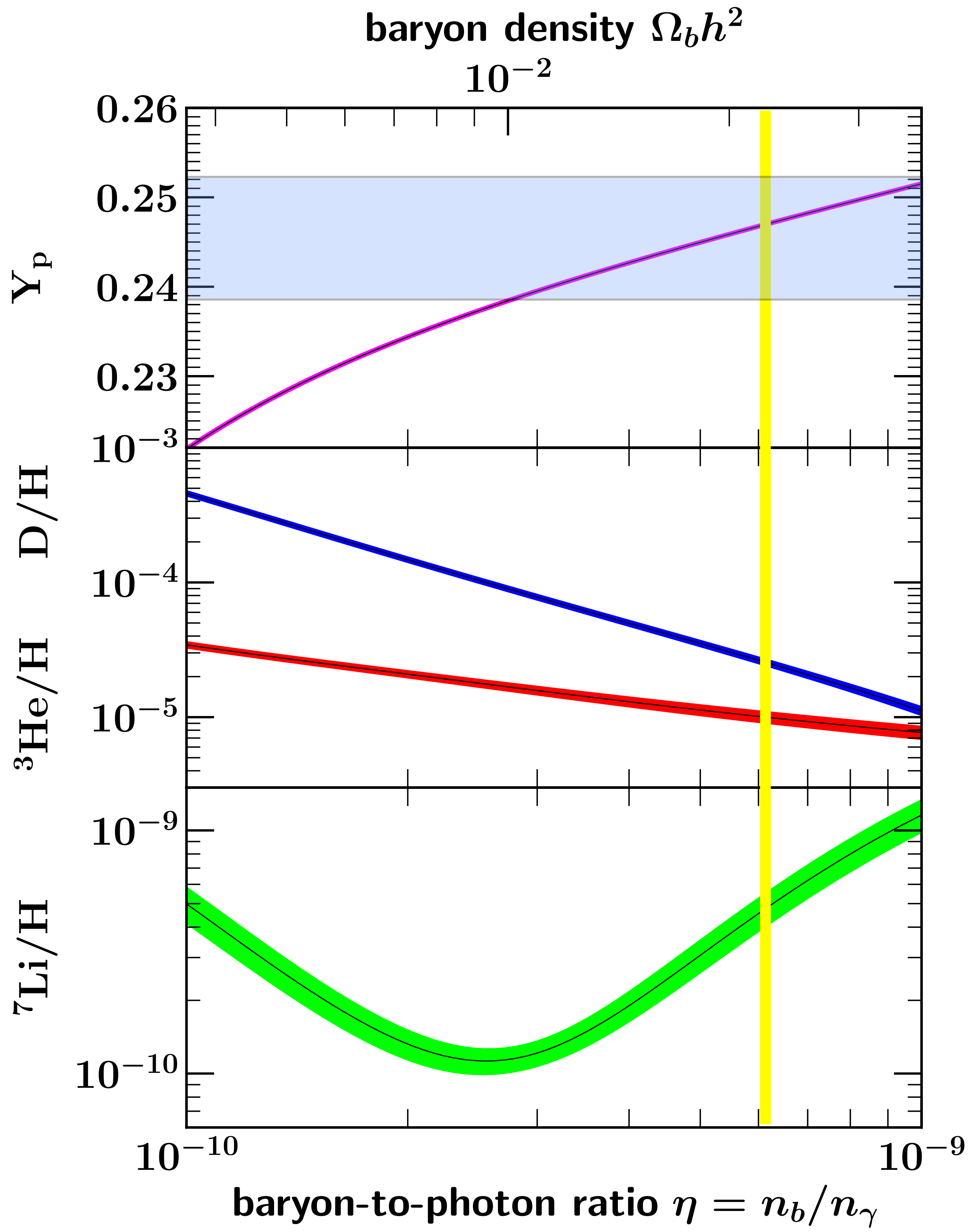

Li/H

Measured in low metallicity dwarf halo stars (over 100 observed)

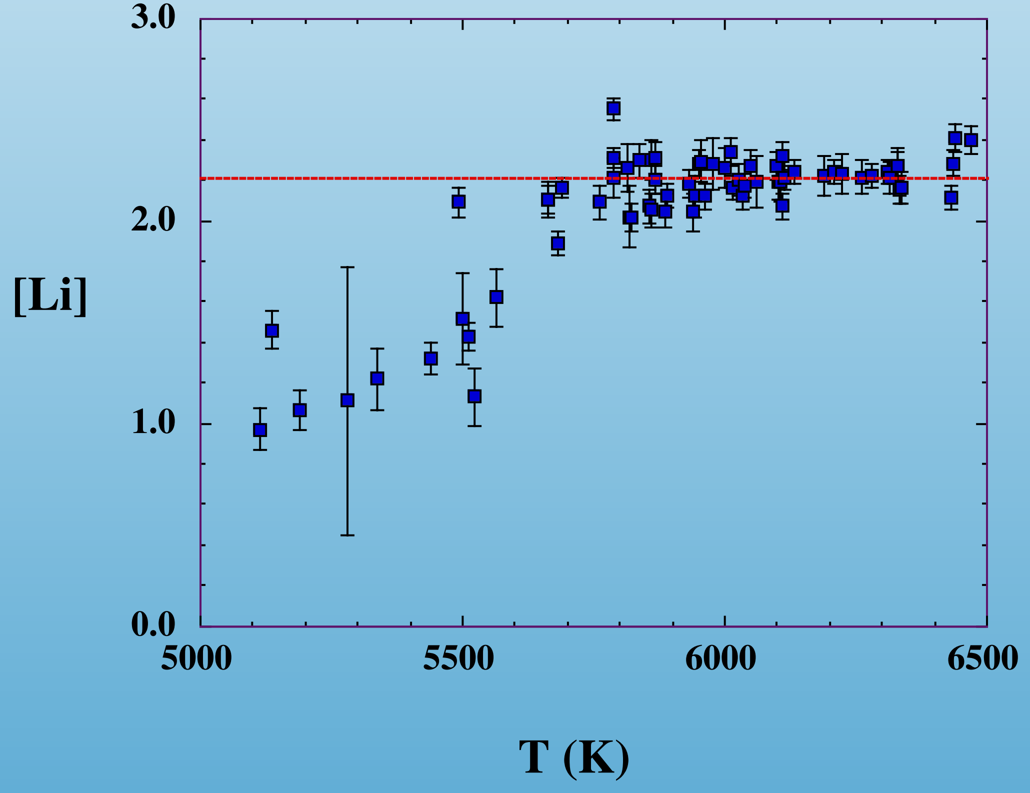

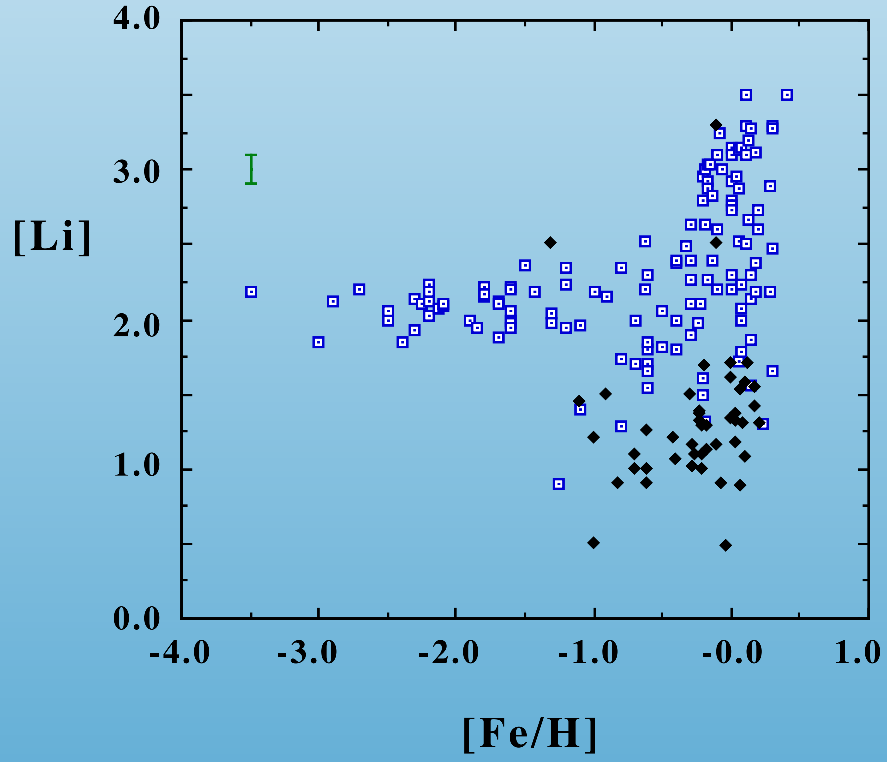

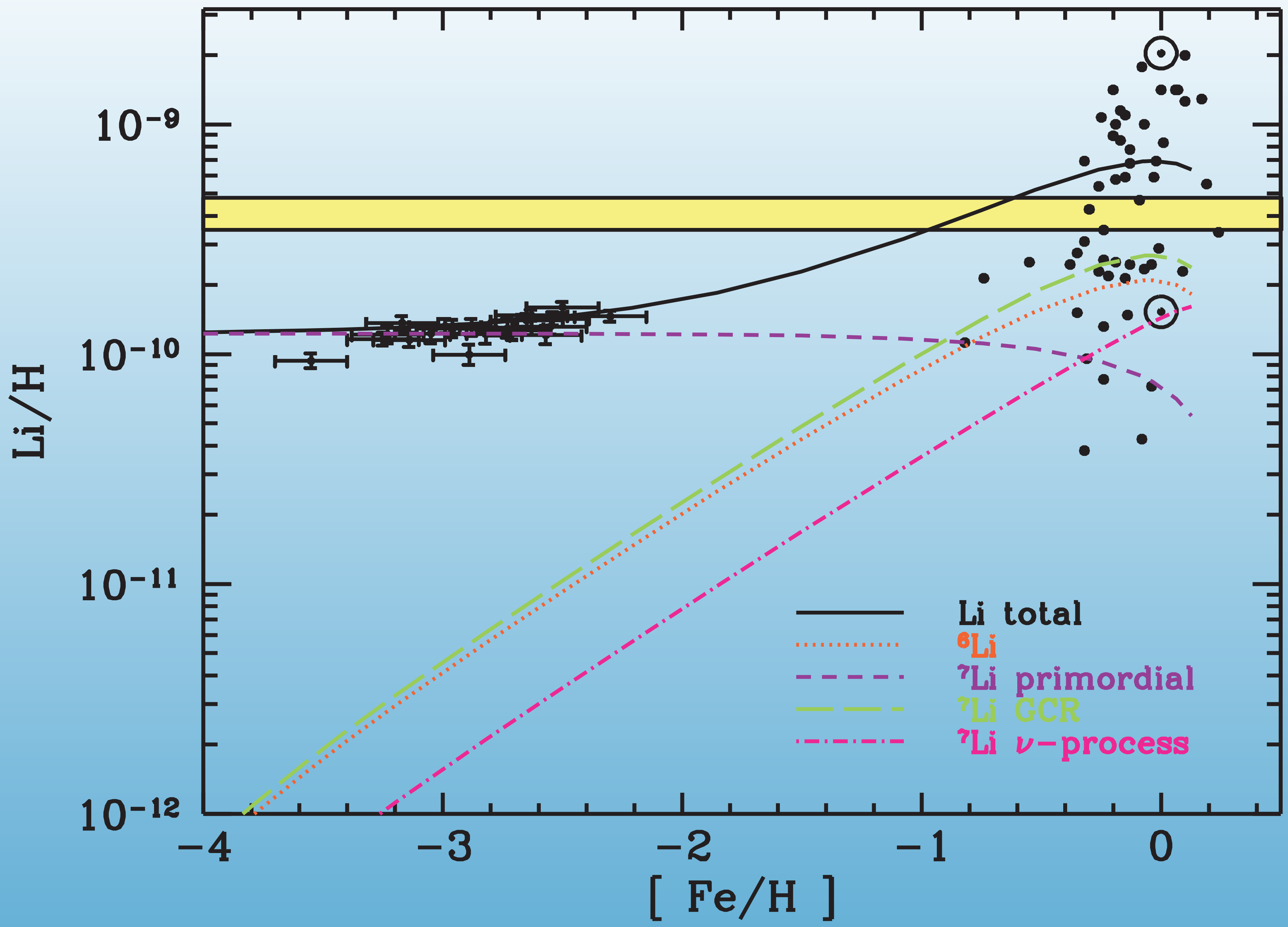

Li/H
[Fe/H]
10−9
10−10
10−11
10−12
−4
−3
−2
−1
0
Li total
6Li
7Li primordial
7Li GCR
7Li ν−process

Possible sources for the discrepancy

- Nuclear Rates/Resonant reactions
- Stellar parameters
- Stellar Depletion

- Decaying Particles
- Axion Cooling
- Variable Constants

Arguments against stellar depletion

- Lack of dispersion in the plateau
- Observation of ^6Li

Broken Spite plateau

Note significant dispersion

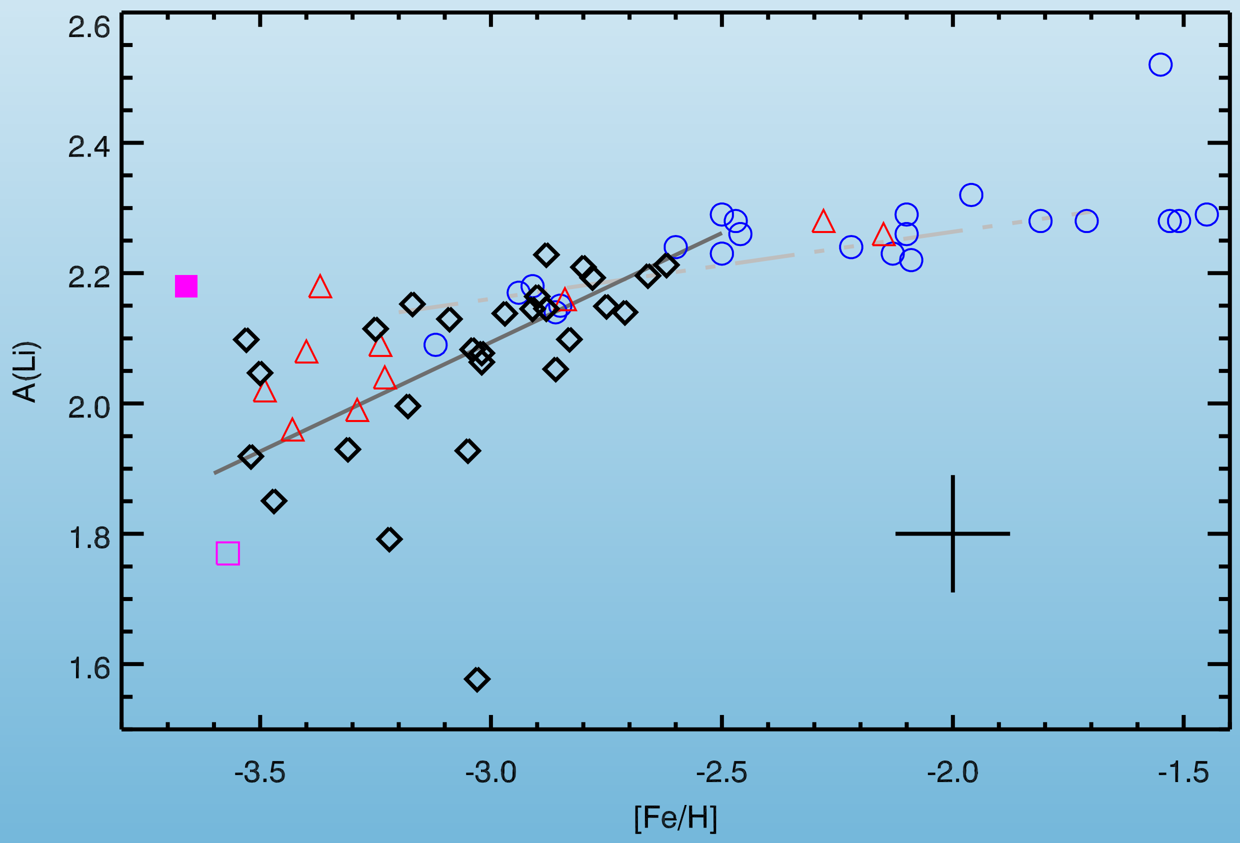

Sbordone et al. (2010)

Broken Spite plateau

Note significant dispersion

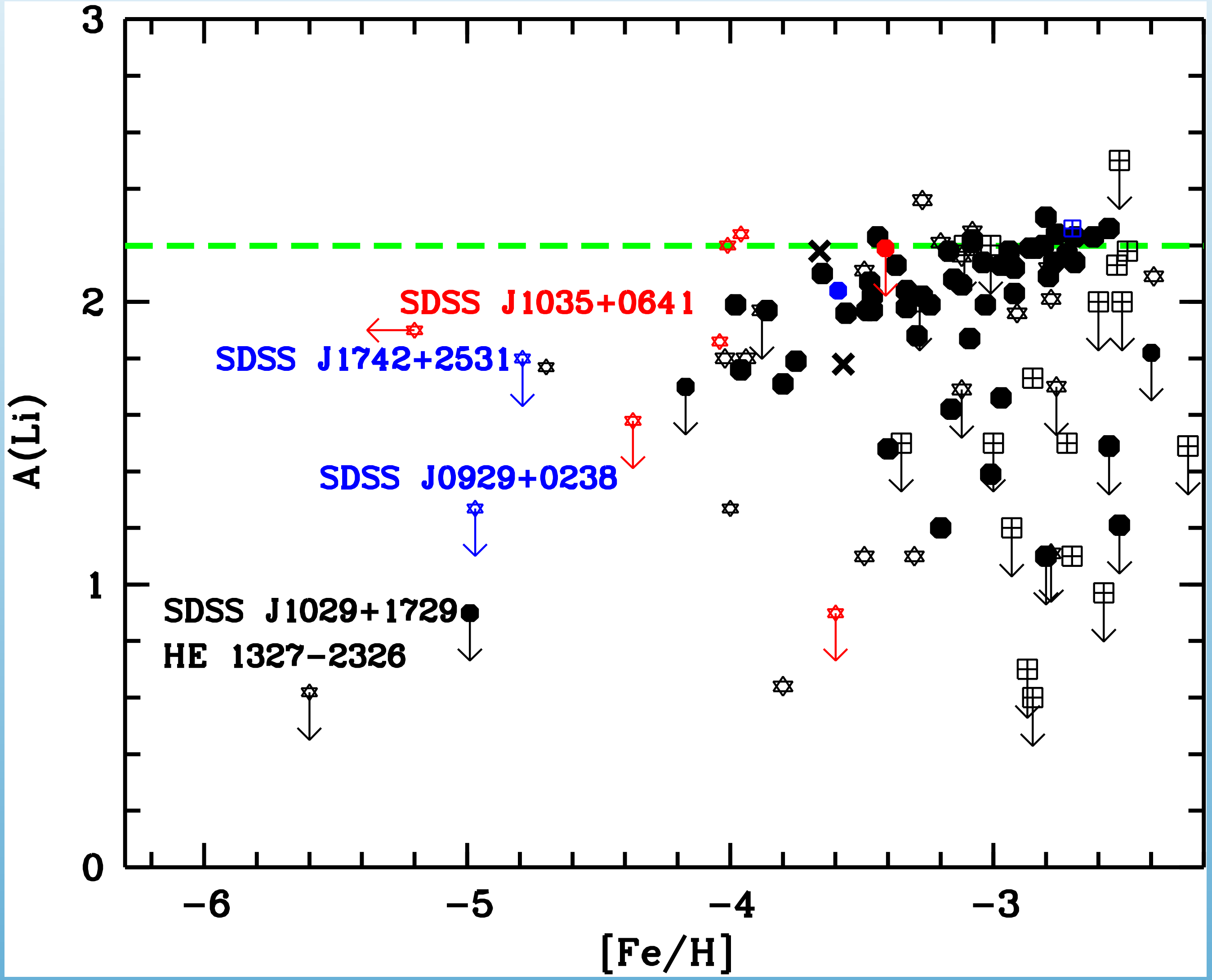

Bonifacio et al. (2018)

Broken Spite plateau

Note significant dispersion

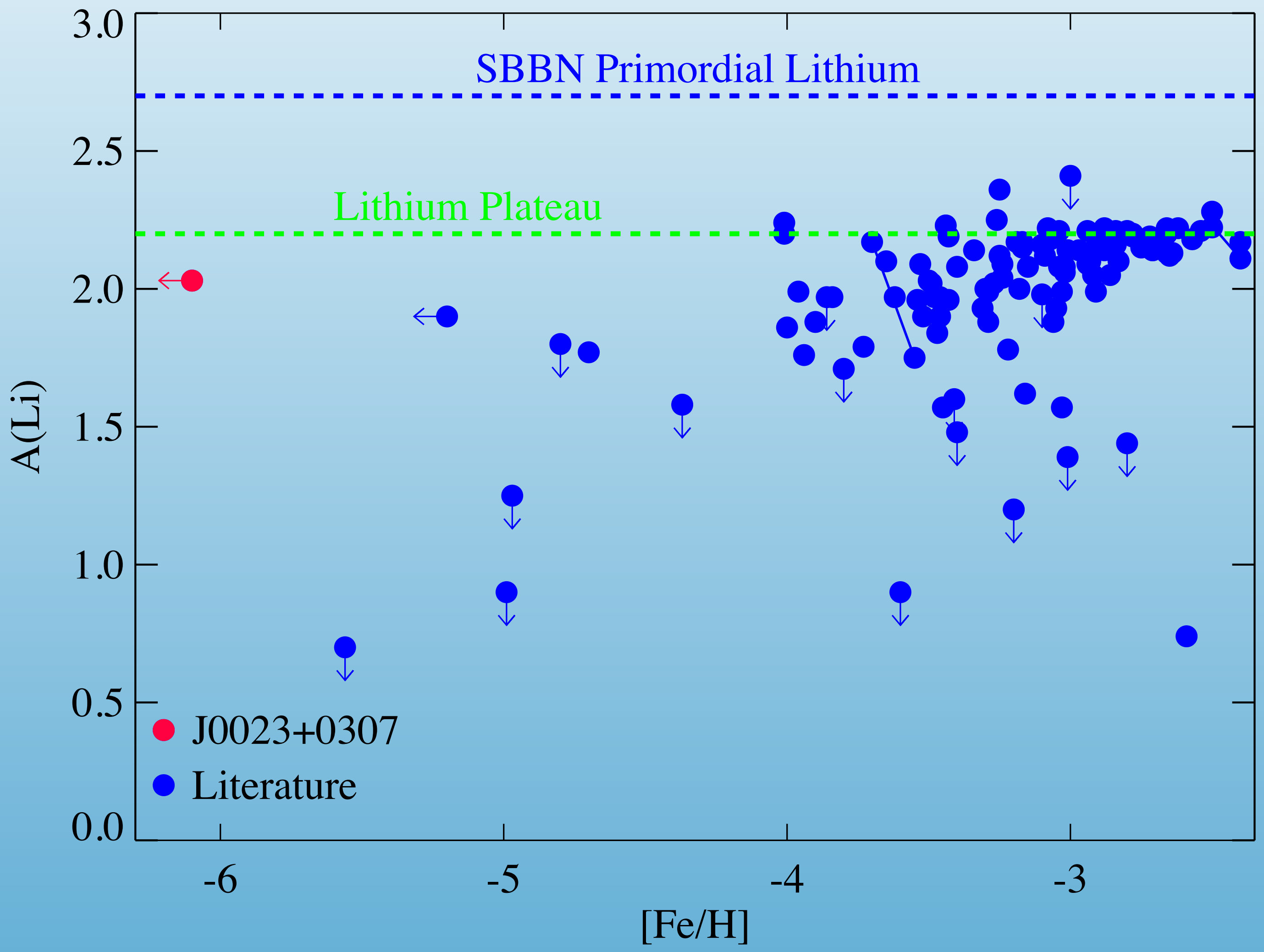

Aguado et al. (2019)

Broken Spite plateau

Note significant dispersion

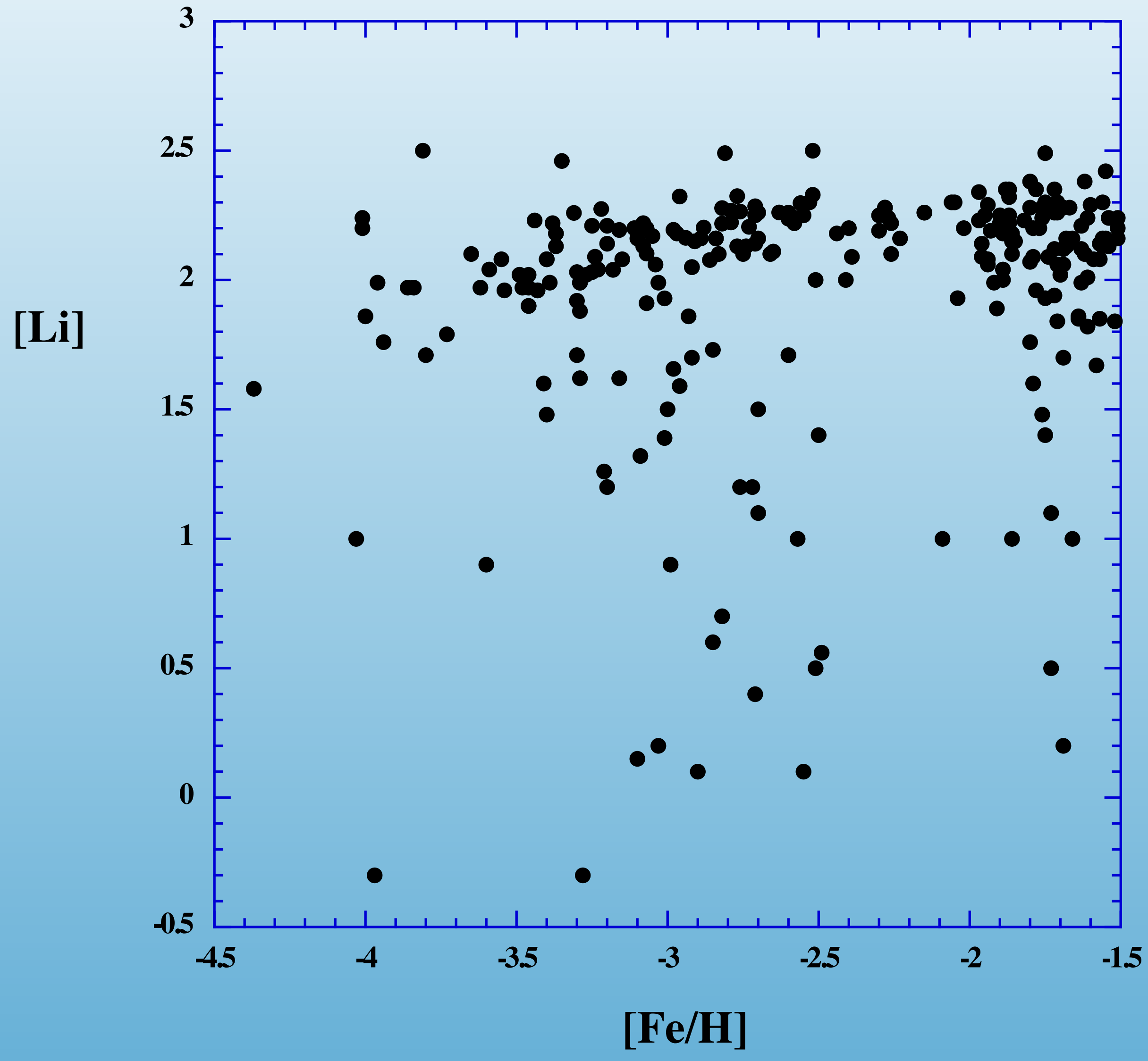

Maybe NO Li Problem

BBN and the CMB

Monte-Carlo approach combining BBN rates, observations and CMB

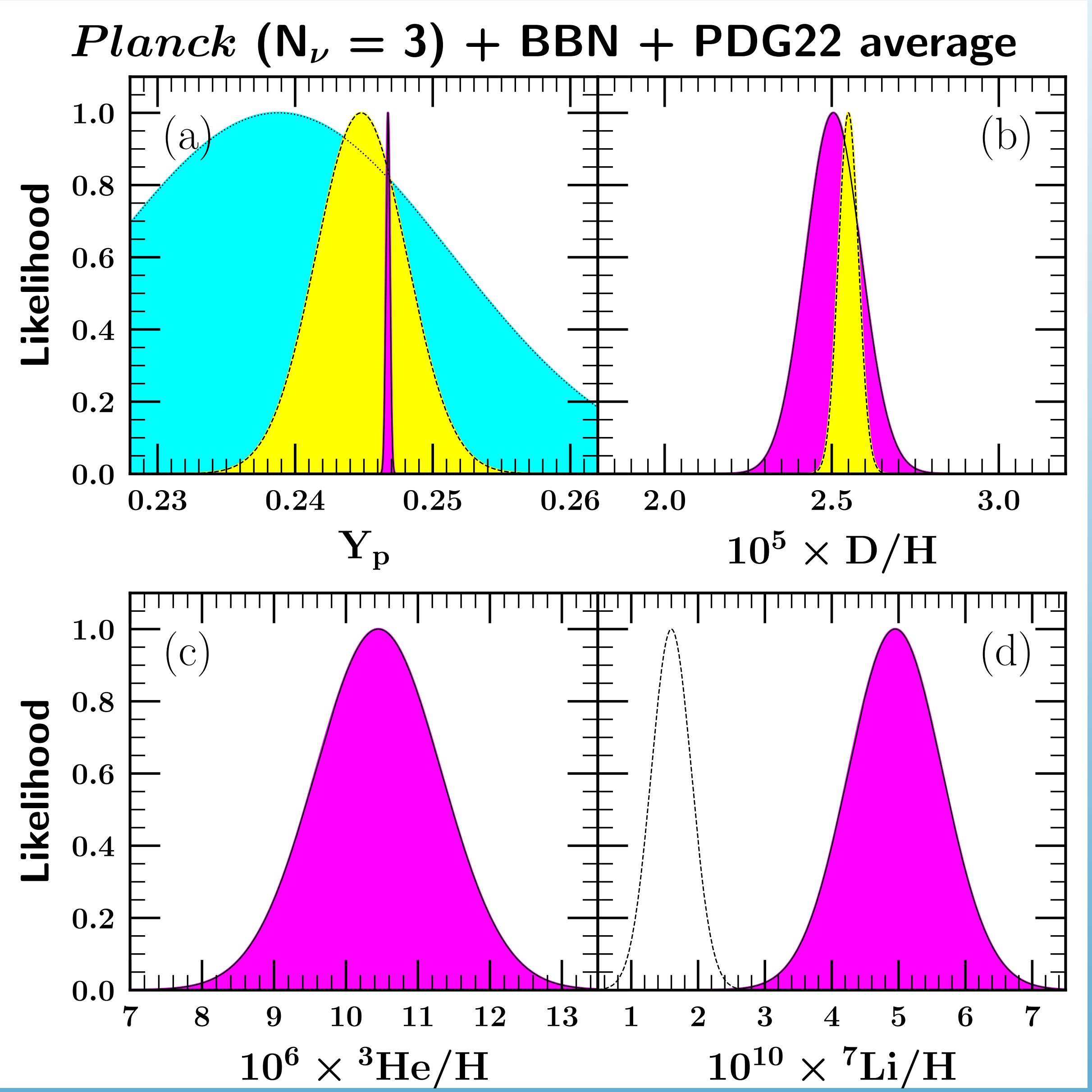

$\mathcal{L}_{\rm OBS}(X)$ Yellow

$$\mathcal{L}_{\rm CMB}(Y_p) \propto \int \mathcal{L}_{\rm CMB}(\eta, Y_p)\, d\eta \,.$$

Cyan

$$\mathcal{L}_{\rm CMB-BBN}(X_i) \propto \int \mathcal{L}_{\rm CMB}(\eta, Y_p)\, \mathcal{L}_{\rm BBN}(\eta; X_i)\, d\eta$$

Purple

Fields, Olive, Yeh, Young

BBN and the CMB

Monte-Carlo approach combining BBN rates, observations and CMB

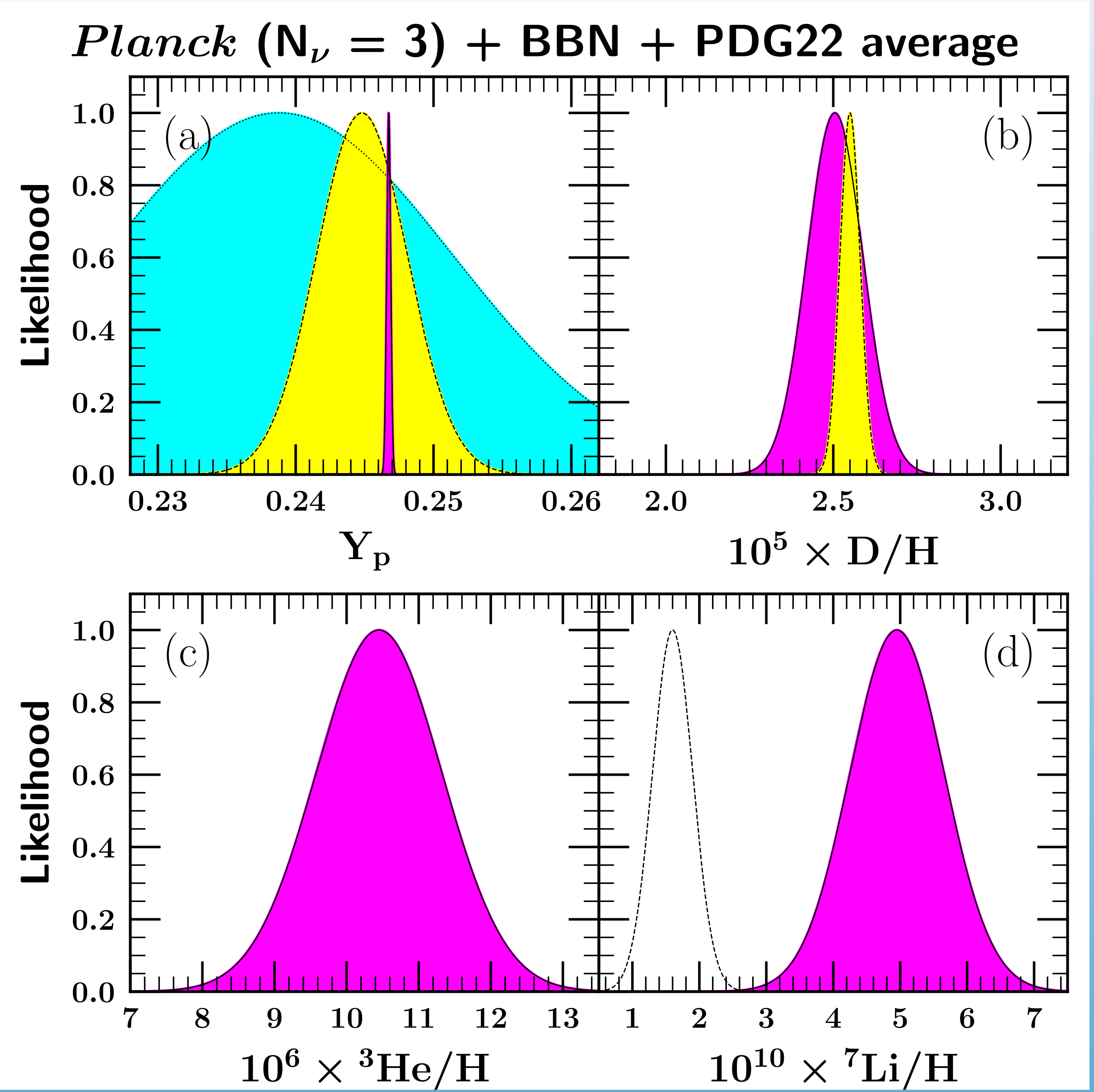

$$
\begin{aligned}
Y_p &= 0.2467 \pm 0.0002 && (0.2467) \\
\mathrm{D/H} &= (2.506 \pm 0.083) \times 10^{-5} && (2.505 \times 10^{-5}) \\
{}^3\mathrm{He/H} &= (10.45 \pm 0.87) \times 10^{-6} && (10.45 \times 10^{-6}) \\
{}^7\mathrm{Li/H} &= (4.96 \pm 0.70) \times 10^{-10} && (4.95 \times 10^{-10})
\end{aligned}
$$

Yeh, Olive, Fields

BBN and the CMB

$N_\nu = 3$

CMB only determination of η and Y_P

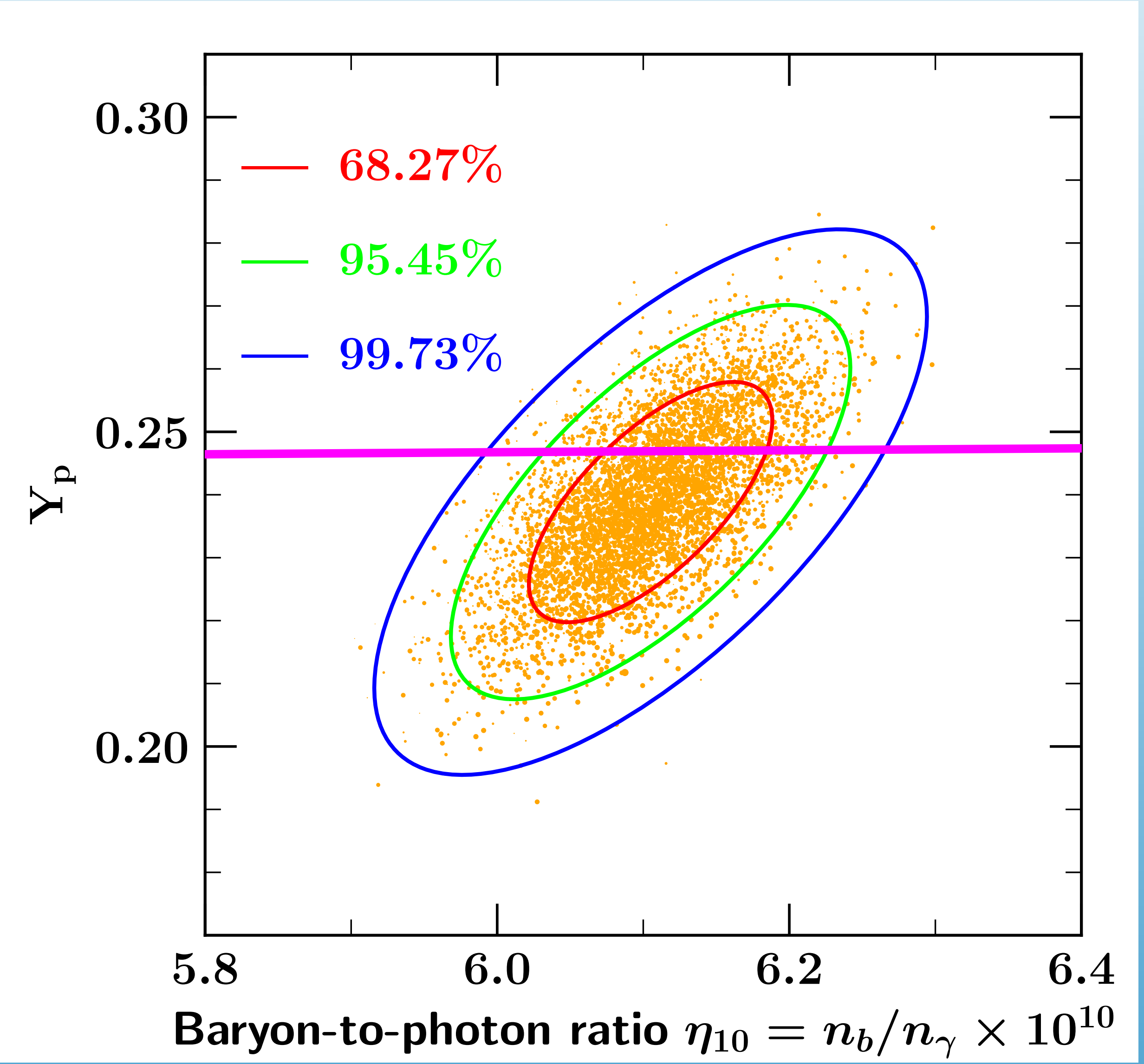

3σ BBN Prediction

Fields, Olive, Yeh, Young

BBN and the CMB

$$\mathcal{L}_{\rm CMB}(\eta) \propto \int \mathcal{L}_{\rm CMB}(\eta, Y_p)\ dY_p\,.$$
$$\mathcal{L}_{\rm CMB-BBN}(\eta) \propto \int \mathcal{L}_{\rm CMB}(\eta, Y_p)\ \mathcal{L}_{\rm BBN}(\eta; Y_p)\ dY_p$$

Convolved Likelihoods

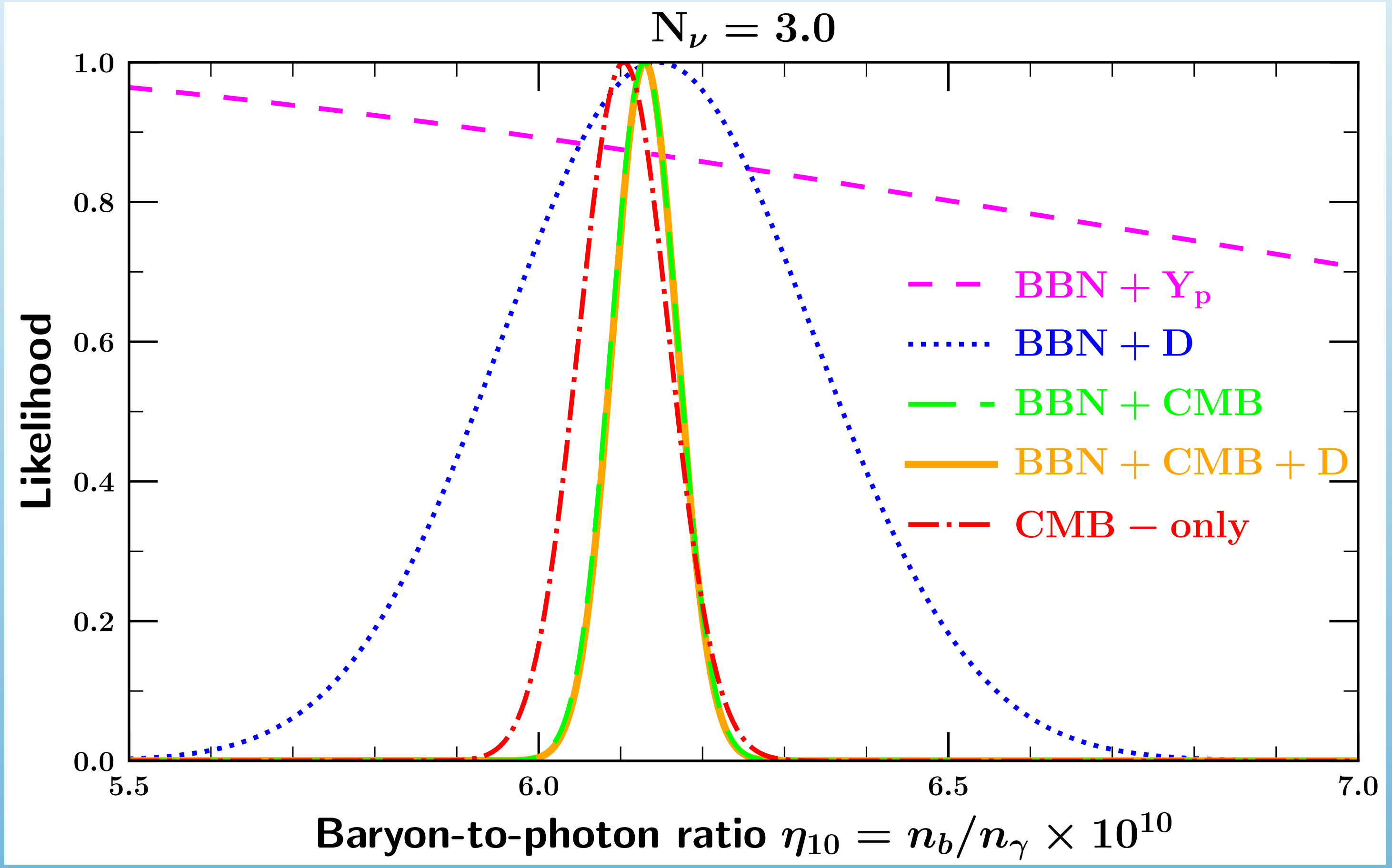

Determination of η

$$\mathcal{L}_{\rm BBN-OBS}(\eta) \propto \int \mathcal{L}_{\rm BBN}(\eta; X_i)\ \mathcal{L}_{\rm OBS}(X_i)\ dX_i$$
$$\mathcal{L}_{\rm CMB-BBN-OBS}(\eta) \propto \int \mathcal{L}_{\rm CMB}(\eta, Y_p)\mathcal{L}_{\rm BBN}(\eta; X_i)\ \mathcal{L}_{\rm OBS}(X_i)\ \prod_i dX_i$$

Fields, Olive, Yeh, Young

BBN and the CMB

Fields, Olive, Yeh, Young

Results for η_{10}

Constraints Used	mean η_{10}	peak η_{10}
CMB-only	6.104 ± 0.055	6.104
BBN+Y_p	$6.741^{+1.220}_{-3.524}$	4.920
BBN+D	6.148 ± 0.191	6.145
BBN+Y_p+D	6.143 ± 0.190	6.140
CMB+BBN	6.129 ± 0.041	6.129
CMB+BBN+Y_p	6.128 ± 0.041	6.128
CMB+BBN+D	6.130 ± 0.040	6.129
CMB+BBN+Y_p+D	6.129 ± 0.040	6.129

Convolved Likelihoods

$$\mathcal{L}_{\rm CMB}(\eta) \propto \int \mathcal{L}_{\rm CMB}(\eta, Y_p)\ dY_p\,.$$

$$\mathcal{L}_{\rm CMB-BBN}(\eta) \propto \int \mathcal{L}_{\rm CMB}(\eta, Y_p)\ \mathcal{L}_{\rm BBN}(\eta; Y_p)\ dY_p$$

$$\mathcal{L}_{\rm BBN-OBS}(\eta) \propto \int \mathcal{L}_{\rm BBN}(\eta; X_i)\ \mathcal{L}_{\rm OBS}(X_i)\ dX_i$$

$$\mathcal{L}_{\rm CMB-BBN-OBS}(\eta) \propto \int \mathcal{L}_{\rm CMB}(\eta, Y_p)\mathcal{L}_{\rm BBN}(\eta; X_i)\ \mathcal{L}_{\rm OBS}(X_i)\ \prod_i dX_i$$

Limits on Particle Properties

$$G_F^2 T^5 \sim \Gamma_{\rm wk}(T_f) = H(T_f) \sim G_N^{1/2} T^2,$$

$$H^2 = \frac{8\pi}{3} G_N \rho$$

$$\rho = \frac{\pi^2}{30}\left(2 + \frac{7}{2} + \frac{7}{4} N_\nu\right) T^4,$$

$$\frac{n}{p} \sim e^{-\Delta m/T}$$

$$Y \sim \frac{2(n/p)}{1 + (n/p)}$$

- BBN Concordance rests on balance between interaction rates and expansion rate.
- Allows one to set constraints on:
  - Particle Types
  - Particle Interactions
  - Particle Masses
  - Fundamental Parameters: G_N, G_F, α

e.g. $\frac{\Delta\alpha}{\alpha} < \text{few} \times 10^{-4}$

BBN and the CMB

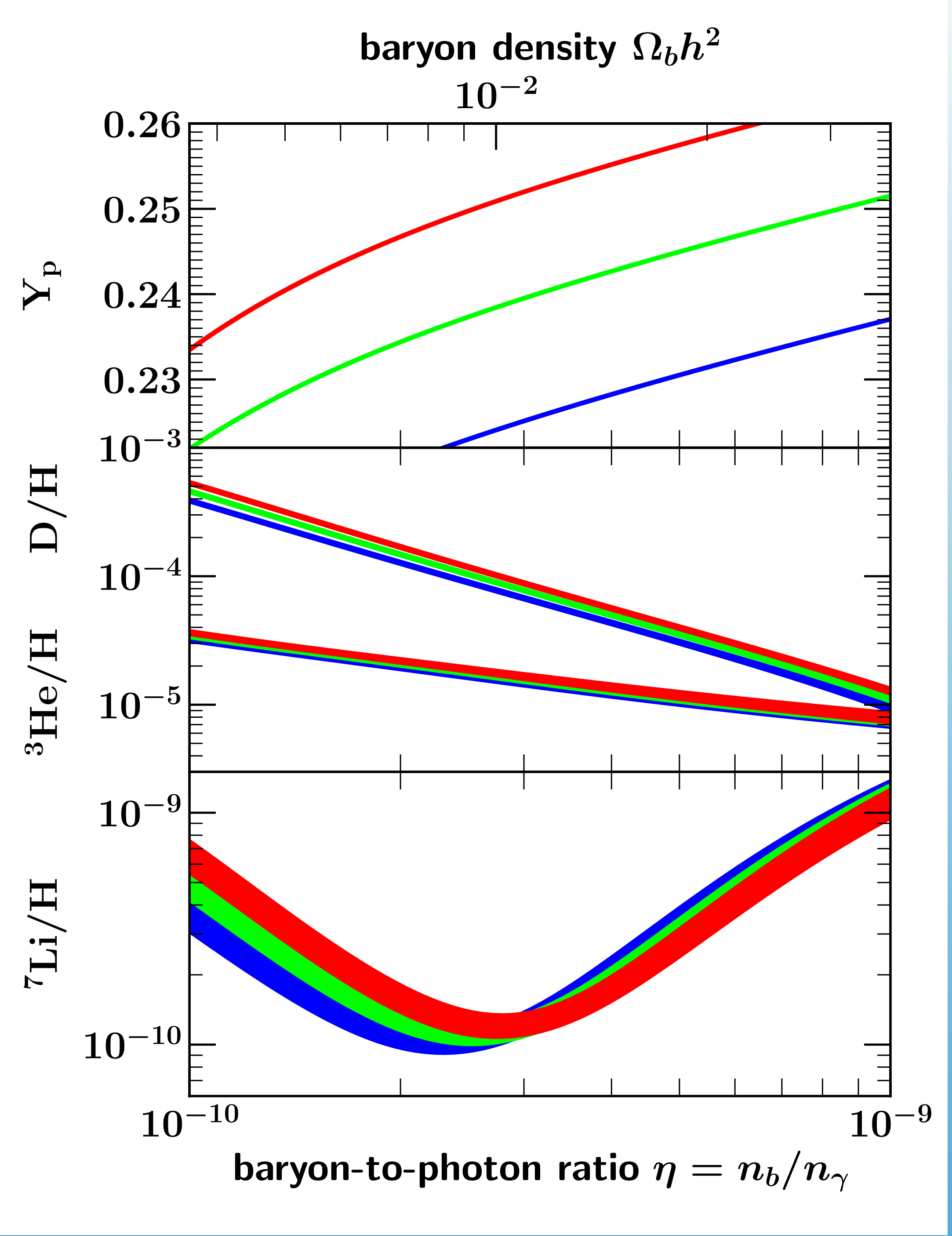

Sensitivity to N_ν

Fields, Olive, Yeh, Young

BBN and the CMB

Monte-Carlo approach combining BBN rates, observations and CMB

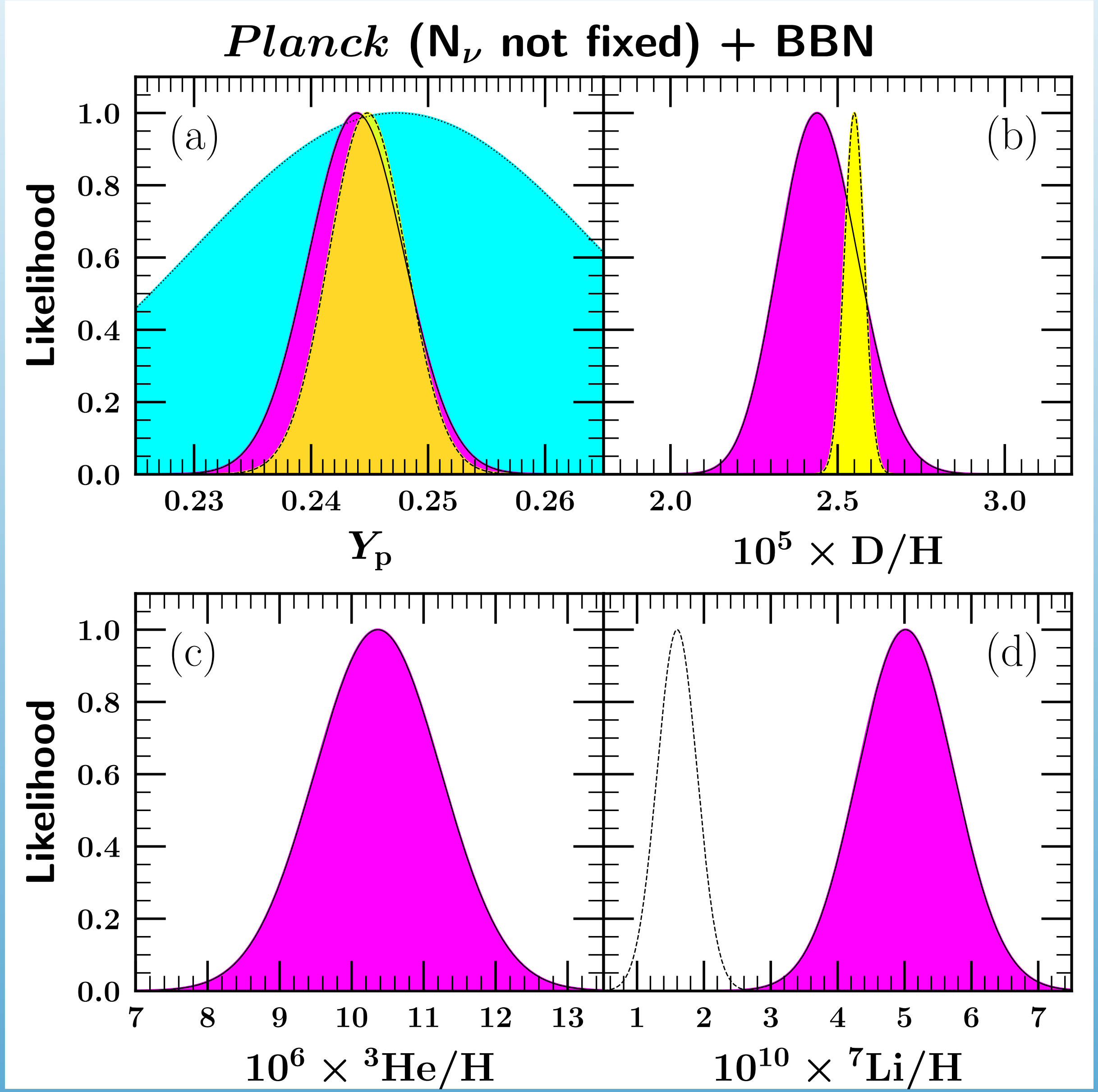

$\mathcal{L}_{\rm OBS}(X)$ Yellow

$$\mathcal{L}_{\rm NCMB}(\eta) \propto \int \mathcal{L}_{\rm NCMB}(\eta, Y_p, N_\nu)\; dY_p\; dN_\nu\,,$$

Cyan

$$\mathcal{L}_{\rm NCMB-NBBN}(\eta) \propto \int \mathcal{L}_{\rm NCMB}(\eta, Y_p, N_\nu)\mathcal{L}_{\rm NBBN}(\eta, N_\nu; X_i)\; dY_p dN_\nu\,,$$

Purple

Fields, Olive, Yeh, Young

BBN and the CMB

CMB and BBN determination of N_ν

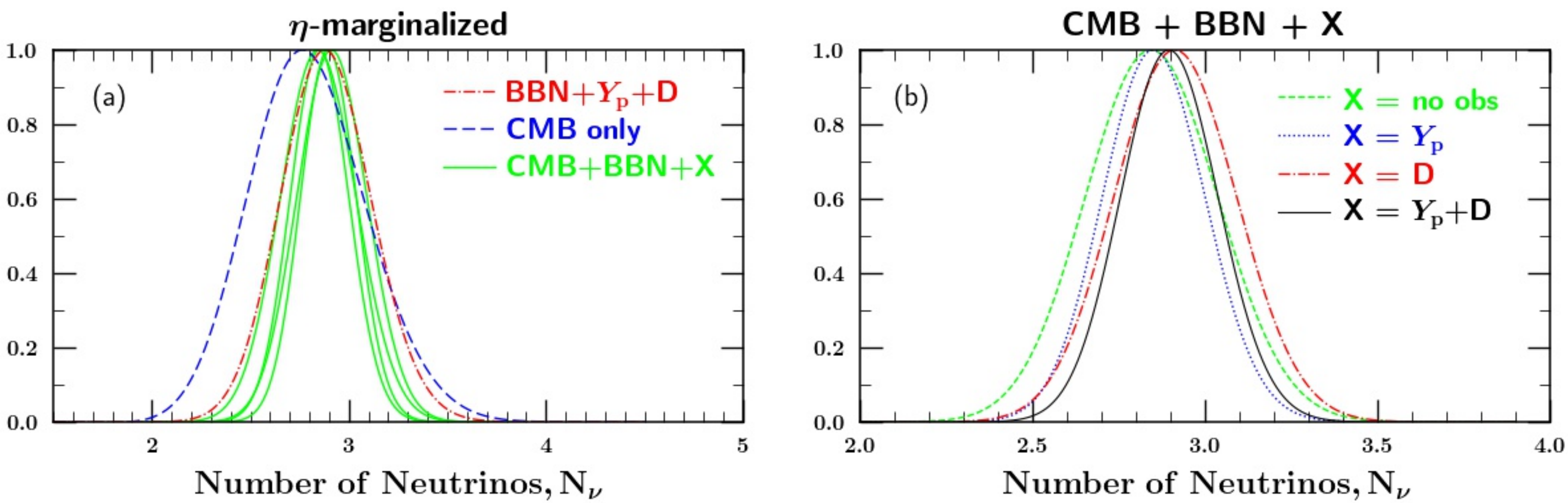

Yeh, Shelton, Olive, Fields

BBN and the CMB

CMB and BBN determination of η and N_ν

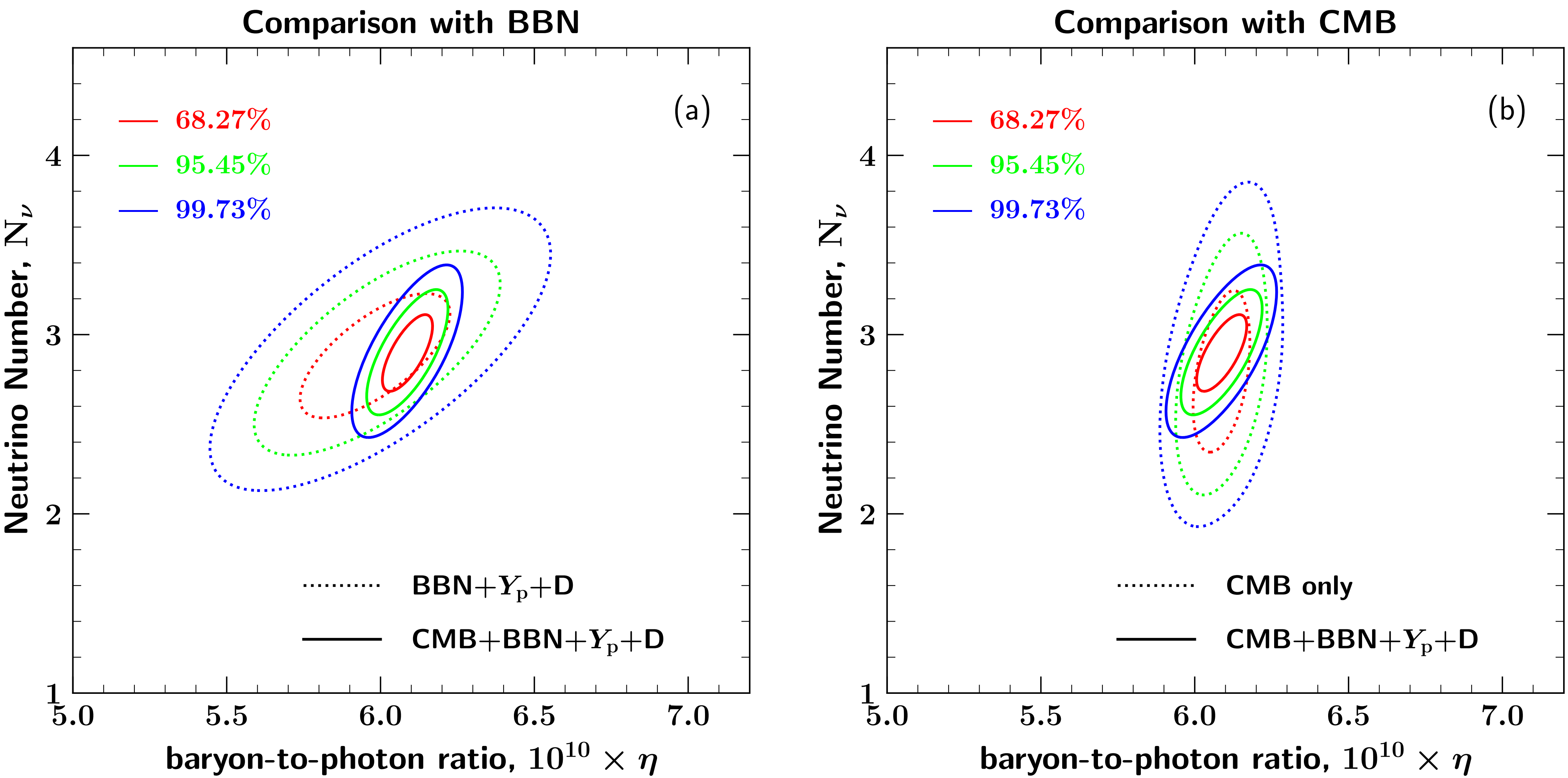

Yeh, Shelton, Olive, Fields

BBN and the CMB

Convolved Likelihoods

Results for η (N_ν)

Constraints Used	mean η_{10}	peak η_{10}	mean N_ν	peak N_ν	δN_ν
CMB-only	6.090 ± 0.061	$6.090^{+0.061}_{-0.062}$	2.800 ± 0.294	$2.764^{+0.308}_{-0.282}$	0.513
BBN+Y_p+D	5.986 ± 0.161	$5.980^{+0.163}_{-0.159}$	2.889 ± 0.229	$2.878^{+0.232}_{-0.226}$	0.407
CMB+BBN	6.087 ± 0.061	$6.088^{+0.061}_{-0.062}$	2.848 ± 0.190	$2.843^{+0.192}_{-0.189}$	0.296
CMB+BBN+Y_p	6.089 ± 0.053	$6.089^{+0.054}_{-0.054}$	2.853 ± 0.148	$2.850^{+0.149}_{-0.148}$	0.221
CMB+BBN+D	6.092 ± 0.060	$6.093^{+0.061}_{-0.060}$	2.916 ± 0.176	$2.912^{+0.178}_{-0.175}$	0.303
CMB+BBN+Y_p+D	6.088 ± 0.054	$6.088^{+0.054}_{-0.054}$	2.898 ± 0.141	$2.895^{+0.142}_{-0.141}$	0.226

Yeh, Shelton, Olive, Fields

BBN and the CMB

Convolved Likelihoods

Results for η (N_ν)

Constraints Used	mean η_{10}	peak η_{10}	mean N_ν	peak N_ν	δN_ν
CMB-only	6.090 ± 0.061	$6.090^{+0.061}_{-0.062}$	2.800 ± 0.294	$2.764^{+0.308}_{-0.282}$	0.513
BBN+Y_p+D	5.986 ± 0.161	$5.980^{+0.163}_{-0.159}$	2.889 ± 0.229	$2.878^{+0.232}_{-0.226}$	0.407
CMB+BBN	6.087 ± 0.061	$6.088^{+0.061}_{-0.062}$	2.848 ± 0.190	$2.843^{+0.192}_{-0.189}$	0.296
CMB+BBN+Y_p	6.089 ± 0.053	$6.089^{+0.054}_{-0.054}$	2.853 ± 0.148	$2.850^{+0.149}_{-0.148}$	0.221
CMB+BBN+D	6.092 ± 0.060	$6.093^{+0.061}_{-0.060}$	2.916 ± 0.176	$2.912^{+0.178}_{-0.175}$	0.303
CMB+BBN+Y_p+D	6.088 ± 0.054	$6.088^{+0.054}_{-0.054}$	2.898 ± 0.141	$2.895^{+0.142}_{-0.141}$	0.226

$N_\nu < 3.180$ (95% CL)

Yeh, Shelton, Olive, Fields

BBN and the CMB

Convolved Likelihoods

Results for η (N_ν)

Constraints Used	mean η_{10}	peak η_{10}	mean N_ν	peak N_ν	δN_ν
CMB-only	6.090 ± 0.061	$6.090^{+0.061}_{-0.062}$	2.800 ± 0.294	$2.764^{+0.308}_{-0.282}$	0.513
BBN+Y_p+D	5.986 ± 0.161	$5.980^{+0.163}_{-0.159}$	2.889 ± 0.229	$2.878^{+0.232}_{-0.226}$	0.407
CMB+BBN	6.087 ± 0.061	$6.088^{+0.061}_{-0.062}$	2.848 ± 0.190	$2.843^{+0.192}_{-0.189}$	0.296
CMB+BBN+Y_p	6.089 ± 0.053	$6.089^{+0.054}_{-0.054}$	2.853 ± 0.148	$2.850^{+0.149}_{-0.148}$	0.221
CMB+BBN+D	6.092 ± 0.060	$6.093^{+0.061}_{-0.060}$	2.916 ± 0.176	$2.912^{+0.178}_{-0.175}$	0.303
CMB+BBN+Y_p+D	6.088 ± 0.054	$6.088^{+0.054}_{-0.054}$	2.898 ± 0.141	$2.895^{+0.142}_{-0.141}$	0.226

$N_\nu < 3.180$ (95% CL)

1-sided limit assuming $N_\nu \geq 3$ $N_\nu < 3.226$ (95% CL)

Yeh, Shelton, Olive, Fields

Limits:

- Right-handed neutrinos and extra gauge boson masses
- Dark Radiation
- Stochastic Gravitational Wave Background
- Vacuum Energy - Trackers
- Primordial Magnetic Fields
- Limits on Changes in η and N_ν between BBN and CMB
- Changes in Fundamental Constants

Yeh, Shelton, Olive, Fields

Summary

- BBN and CMB are in excellent agreement wrt D and He
- Li: Was Problematic
  - Most certainly now due to stellar depletion
- Wish list:
  - New cross sections measurements for D(D,p) and D(D,n)
  - New high precision measurements of He
- Standard Model ($N_\nu = 3$) is looking good!

Neutrino Temperature

- At T ~ 1 MeV neutrinos decouple
- At T ~ 1/2 MeV e^+ e^- annihilate to photons
- Entropy of "γ's" and ν's conserved speparately
- Prior to annihilation, $T_\gamma = T_\nu = T_>$

$$s_> = \frac{4}{3}\frac{\rho_>}{T_>} = \frac{4}{3}(2+\frac{7}{2})(\frac{\pi^2}{30})T_>^3$$

- After annihilation, $T_\gamma = T_<$ but, $T_\nu = T_>$

$$s_< = \frac{4}{3}\frac{\rho_<}{T_<} = \frac{4}{3}(2)(\frac{\pi^2}{30})T_<^3$$

$$T_\nu = (4/11)^{1/3} T_\gamma \simeq 1.9K$$

What does N > 3 mean?

If limit on $\Delta N < 0.226$

and $\Delta N_\nu = 3$

$$3\left(\frac{T_{\Delta N}}{T_\nu}\right)^4 < .226 \implies \left(\frac{T_{\Delta N}}{T_\nu}\right)^3 < 0.14$$

$$\left(\frac{T_{\Delta N}}{T_\nu}\right)^3 = \frac{43}{4g*}$$

$$g* > 75$$

What does N > 3 mean?

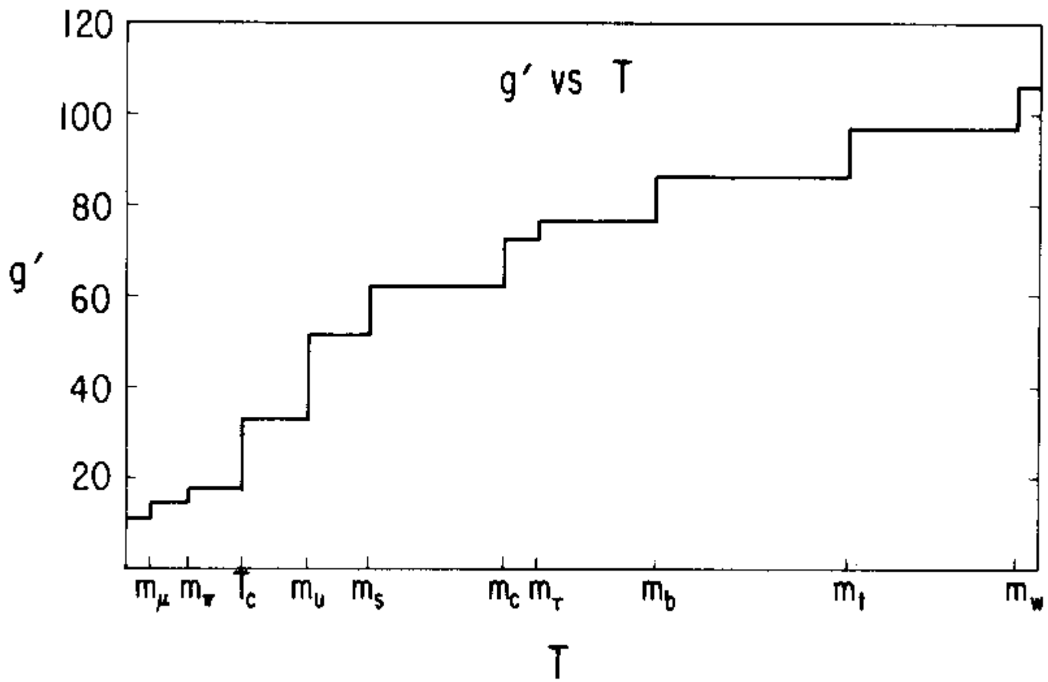

Need $T_f > m_\tau$

What does N > 3 mean?

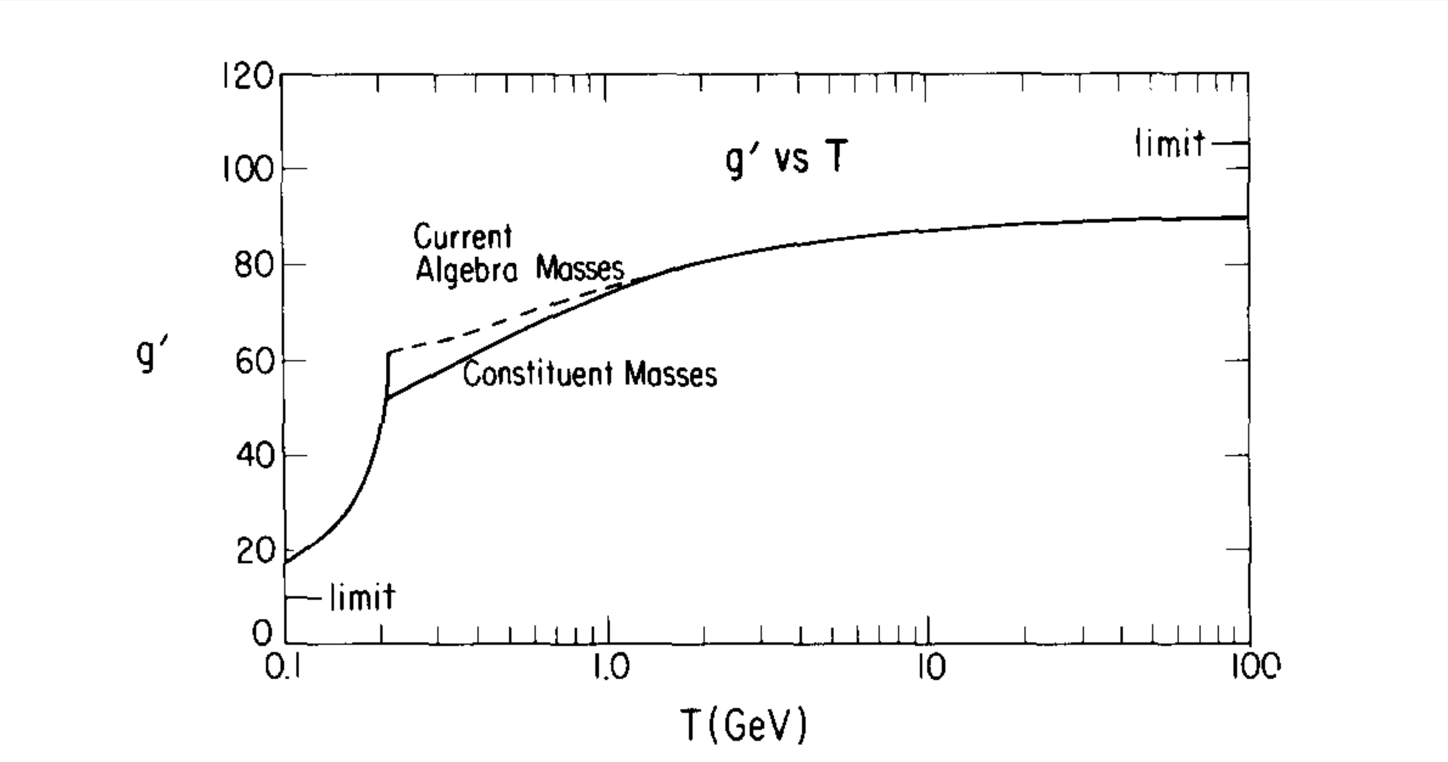

What does N > 3 mean?

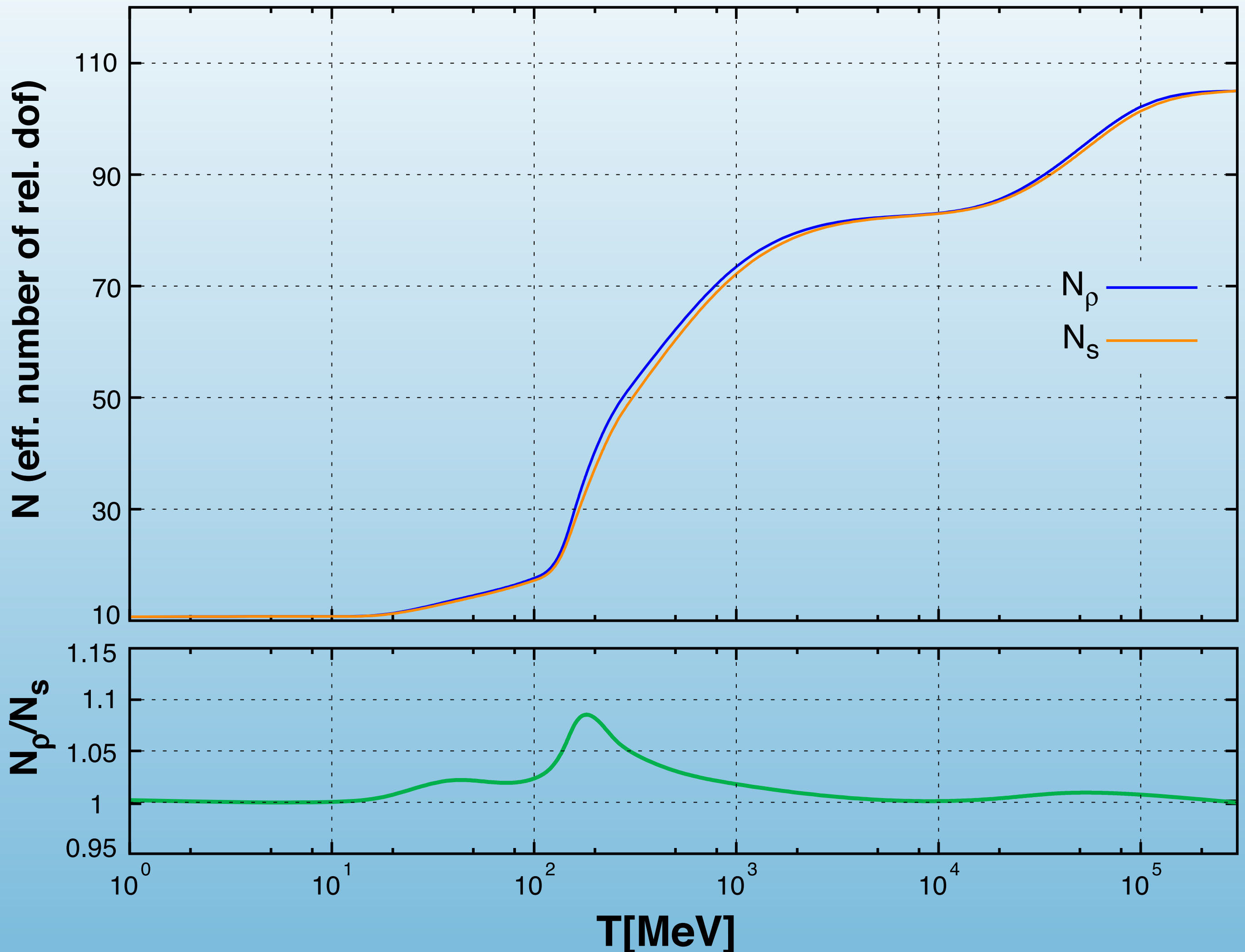

Need $T_f > 1.2$ GeV

Borsanyi et al. 2016

What does N > 3 mean?

Today,

$$\rho_{rad} = \frac{\pi^2}{30}\left(2 + \frac{7}{4}N_\nu(\frac{T_\nu}{T_\gamma})^4\right)T_\gamma^4$$

$$= \frac{\pi^2}{30}\left(2 + \frac{21}{4}(\frac{4}{11})^{4/3} + \frac{7}{4}\Delta N(\frac{T_{\Delta N}}{T_\gamma})^4\right)T_\gamma^4$$

Scalars: $\Delta N = 4/7$

Dirac Fermion: $\Delta N = 2$